

KLIWAS Schriftenreihe KLIWAS-63/2014

**On the coupling of the oceanic North Sea
model HAMSOM with the regional
atmospheric model REMO**

Koblenz, im März 2014



BUNDESAMT FÜR
SEESCHIFFFAHRT
UND
HYDROGRAPHIE

CSC
Climate Service Center
Germany



Eine Einrichtung des Helmholtz-Zentrums Geesthacht



KLIWAS

**KLIWAS Schriftenreihe
KLIWAS-63/2014**

**On the coupling of the oceanic North Sea
model HAMSOM with the regional
atmospheric model REMO**

**Autoren:
Christopher Moseley
Daniela Jacob**

**A cooperation of
Bundesamt für Seeschifffahrt und
Hydrographie and
Helmholtz-Zentrum-Geesthacht /
Climate Service Center**

Page
Chapter

Contents

04		LIST OF FIGURES
05		LIST OF TABLES
07	1	INTRODUCTION
09	2	AVAILABLE MODEL SIMULATIONS
12	3	OBSERVATIONAL DATASETS
14	4	VALIDATION OF THE REMO SIMULATIONS WITH OBSERVATIONAL DATA
14	4.1	SEA SURFACE TEMPERATURE AND SEA ICE COVER
17	4.2	NEAR SURFACE AIR TEMPERATURE
19	4.3	PRECIPITATION
21	4.4	EVAPORATION
23	4.5	CLOUD COVER
25	4.6	SEA LEVEL PRESSURE
27	4.7	SURFACE FLUXES
30	4.8	RADIATION
32	5	ESTIMATION OF THE REMO SIMULATIONS WITHIN THE BANDWIDTH OF THE ENSEMBLES REGIONAL MODEL SIMULATIONS
46	6	COMPARISON OF THE COUPLED REMO/HAMSOM SIMULATION WITH THE OTHER REMO SIMULATIONS OVER THE NORTH SEA REGION
52	7	CONCLUSION
54		REFERENCES

Page

Figure

List of Figures

09	1	REMO DOMAIN AND MPIO M GRID
15	2	MEAN SST OF ERA40 FOR THE PERIOD 1961-2000, SST DIFFERENCE OF CSC-022 TO ERA40, SST DIFFERENCE OF MPI-253 AND IFM-002 TO ERA40 AND SST DIFFERENCE OF HOAPS AND NOCS TO ERA40 IN THE PERIOD 1987-1999
16	3	TIME DEVELOPMENT OF AREA AVERAGED SST OVER THE NORTH SEA FOR ERA40, BSH OBSERVATIONAL DATASET, MARSDIEP IN SITU MEASUREMENT, SIMULATION WITH NCEP DRIVEN UNCOUPLED MPIO M AND SIMULATION MPI-253
17	4	SEA ICE COVER OF ERA40 [%], DIFFERENCE IN SEA ICE COVER BETWEEN SIMULATION MPI-253 TO ERA40, DIFFERENCE IN SEA ICE COVER BETWEEN NCEP AND NOCS TO ERA40
18	5	DIFFERENCES IN 2M TEMPERATURE TO ERA40 [°C] FOR THE PERIOD 1961-2000
20	6	YEARLY MEAN PRECIPITATION [MM/D] OF ERA40 (1961-2000), AND DIFFERENCE OF NCEP (1961-2000), AND HOAPS (1987-1999) TO ERA40
22	7	DIFFERENCES IN EVAPORATION TO ERA40 [MM/D] FOR THE PERIOD 1961-2000 FOR MPI-253 (1961-2000), CSC-022 (1961-2000), CSC-300 (1961-2000) AND HOAPS (1987-1999)
24	8	CLOUD COVER FRACTION [%] OF ERA40 DATASET, MEAN 1961-2000 AND DIFFERENCE OF NOCS AND ERA40 CLOUD COVER (OCEAN ONLY), MEAN OVER 1986-1999
26	9	YEARLY MEAN SEA LEVEL PRESSURE [HPA] OF ERA40 (1961-2000), AND DIFFERENCE OF NCEP (1961-2000), AND NOCS (1987-1999)
28	10	YEARLY MEAN LATENT HEAT FLUX [W/M²] OF NCEP (1961-2000), AND DIFFERENCE OF HOAPS AND NOCS (1987-1999) TO NCEP. DIFFERENCE IN MEAN LATENT HEAT FLUX OF REMO SIMULATIONS MPI-253, CSC-022 AND CSC-300 TO NCEP (1961-2000)
29	11	YEARLY MEAN SENSIBLE HEAT FLUX [W/M²] OF NCEP (1961-2000), AND DIFFERENCE OF HOAPS AND NOCS (1987-1999) TO NCEP. DIFFERENCE IN MEAN SENSIBLE HEAT FLUX OF REMO SIMULATIONS MPI-253, CSC-022 AND CSC-300 TO NCEP (1961-2000)
31	12	YEARLY MEAN NET SURFACE SOLAR RADIATION [W/M²] OF NCEP (1961-2000), AND DIFFERENCE OF ERA40 (1961-2000) AND NOCS (1987-1999) TO NCEP
31	13	DIFFERENCE IN YEARLY MEAN NET SURFACE THERMAL RADIATION [W/M²] OF ERA40 (1961-2000), HOAPS, AND NOCS (1987-1999) TO NCEP
33	14	MAP OF THE FOUR DOMAINS OF THE NORTH SEA, USED FOR AVERAGING

Page	Figure	
36	15	THE BOX-AND-WHISKER SHOW THE BANDWIDTH OF THE ENSMBLES HINDCAST SIMULATIONS FOR THE 2M AIR TEMPERATURE [°C], AVERAGED OVER THE PERIOD 1961-2000 AND OVER THE FOUR DOMAINS OF THE NORTH SEA AS SHOWN IN FIG. 14
37	16	SIMILAR AS FIG. 15, FOR 2M DEW POINT TEMPERATURE [°C]
38	17	SIMILAR AS FIG. 15, FOR PRECIPITATION [MM/D]
39	18	SIMILAR AS FIG. 15, FOR EVAPORATION [MM/D]
40	19	SIMILAR AS FIG. 15, FOR CLOUD COVER [%]
41	20	SIMILAR AS FIG. 15, FOR MEAN SEA LEVEL PRESSURE [HPA]
42	21	SIMILAR AS FIG. 15, FOR LATENT HEAT FLUX [W/M2]
43	22	SIMILAR AS FIG. 15, FOR SENSIBLE HEAT FLUX [W/M2]
44	23	SIMILAR AS FIG. 15, FOR NET SURFACE SOLAR RADIATION [W/M2]
45	24	SIMILAR AS FIG. 15, FOR NET SURFACE THERMAL RADIATION [W/M2]
48	25	SEA SURFACE TEMPERATURE DIFFERENCE BETWEEN IFM-201 AND MPI-253 [°C]
49	26	2M AIR TEMPERATURE DIFFERENCE BETWEEN IFM-201 AND MPI-253 AND IFM-123 AND MPI-253 [°C]
49	27	EVAPORATION DIFFERENCE BETWEEN IFM-201 AND MPI-253 AND IFM-123 AND MPI-253 [MM/D]
50	28	LATENT HEAT FLUX DIFFERENCE BETWEEN IFM-201 AND MPI-253 AND IFM-123 AND MPI-253 [W/M2]
50	29	SENSIBLE HEAT FLUX DIFFERENCE BETWEEN IFM-201 AND MPI-253 AND IFM-123 AND MPI-253 (BOTTOM) [W/M2]
51	30	SURFACE THERMAL RADIATION DIFFERENCE BETWEEN IFM-201 AND MPI-253 AND IFM-123 AND MPI-253 [W/M2]

Page	Table	
------	-------	--

List of Tables

11	1	OVERVIEW OVER THE SIMULATIONS EVALUATED WITHIN THIS REPORT
13	2	AVAILABLE DATASETS

1 Introduction

The aim of the cooperation between BSH and CSC of Helmholtz-Zentrum Geesthacht within the context of the KLIWAS project is to provide a model basis for the description of the climate of the North Sea region as a foundation for the study of future climate changes. It has been realized that regional coupled atmosphere-ocean models are crucial for the study of maritime regions. Without them, a reliable assessment of changes in the economic use and coastal protection is not possible. Therefore, the project 2.01 within KLIWAS develops a coupled regional climate model for the North Sea in cooperation with the „Institut für Meereskunde“ (IfM) of the University of Hamburg, and the Max-Planck-Institut für Meteorology (MPI), in order to extend the ensemble of existing uncoupled regional climate projections. For this purpose, the regional ocean model HAMSOM, developed by IfM (Pohlmann, 2006), has been coupled to the atmospheric model REMO (Su et al. 2013), developed by MPI and CSC. Previously, the ocean model of MPI, the global MPIOM, has been coupled to REMO in a similar way (Sein et al., 2013).

Before the scenario simulations of the planned climate projections could begin, the coupled models had to be validated with the observed climate of the past 30 to 50 years. Therefore MPI and IfM performed uncoupled as well as coupled „hindcast“ simulations, which are driven by reanalysis data (NCEP for the atmosphere and GECCO for the ocean). Since an atmospheric model (REMO) and two ocean models (the global MPIOM and the regional HAMSOM) are involved in these simulations, a large number of coupled and uncoupled simulations are possible, out of which only a selection could actually be performed. Both the coupled REMO/MPIOM and REMO/HAMSOM models contributed to the selected simulation ensemble and appropriate model domains have been chosen. CSC complemented the simulations of MPI and IfM by an uncoupled REMO simulation with NCEP forcing at the lateral boundaries and at the sea surface, which was still missing in the ensemble. To assess the utility of the model configurations for the aims of KLIWAS and to analyze the performance of the models, the hindcast simulations have been evaluated and compared among each other. Further, the simulations were validated against observational datasets, in order to estimate the model biases. A similar analysis for the North Sea and Baltic Sea region was previously given by Schrum et al. (2003). It was agreed not to bias correct the model simulations, to avoid a disturbance of the internal consistency of the uncoupled and coupled simulations.

The main contribution of CSC to the project was the evaluation of the atmospheric variables of the simulations, the assistance for the coupling, and the performance of an additional simulation with REMO. Evaluation of the oceanic data was not part of the CSC work, but was done by the project partners. CSC joined the KLIWAS

meetings at on 3/4 March 2012 at SMHI, on 3-4 December 2013, and on 28/29 May 2013 to present the status of the results. Further, CSC organized several meetings with the partners of BSH, IfM, and MPI, to discuss the state of the work and agree on the further procedure of the model simulations and the evaluation, and to stay in regular contact with the partners.

This report is organized as follows: Chapter 2 describes the different simulations and model setups, and Chapter 3 lists the reanalysis and observational datasets used for the validation. Results of the validation are presented in Chapter 4, results of an inter-comparison with the simulations provided by the ENSMBLES database is given in Chapter 5, and the effect of the REMO-HAMSOM coupling is provided in Chapter 6. Chapter 7 gives a conclusion.

2 Available model simulations

The model simulations used for the following evaluation consist of simulations with REMO stand-alone, simulations with REMO coupled with MPIOM, and REMO coupled with HAMSOM (Su et al. 2013). MPI-M, IfM, and CSC performed them. A description of the REMO and MPIOM models, as well as their coupling, is given in Sein et al. (2013).

The model domains of REMO and HAMSOM are shown in Fig. 1. The REMO simulations are set up with a horizontal resolution of 30 km (181x181 grid boxes), while HAMSOM is run at a higher horizontal resolution of 3 km on a smaller domain. The model domain of MPIOM is the entire globe. For the calculation of the fluxes, REMO needs the state of the sea surface as input, as the SST and the sea ice concentration. These input variables can either be prescribed by given datasets in the uncoupled case, or given by a coupled ocean model (HAMSOM or MPIOM). Correspondingly, the ocean models need the state of the lowest atmospheric layer, which are either provided by a reanalysis data set, or by REMO in the coupled case.

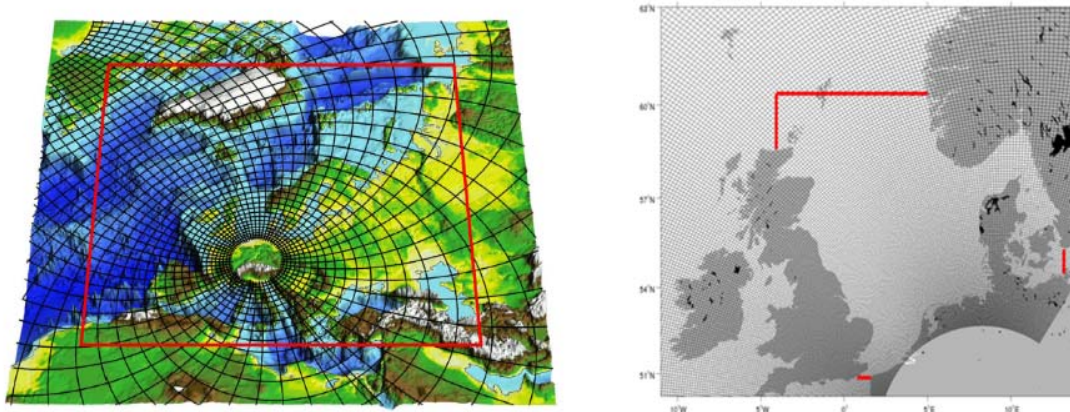


Figure 1: Left: REMO domain and MPIOM grid. Right: HAMSOM domain. Figure provided by IfM.

All model simulations used for the evaluation are named by the institution by which they were performed, and their run number. In the following, a description of the model setup of every individual simulation is given:

CSC-022 (1958-2001):

Uncoupled REMO simulation with NCEP reanalysis forcing (SST and atmospheric lateral boundaries). The sea ice cover was taken from the ERA40 reanalysis, since it was already prepared and tested as forcing for REMO, such that an extensive preparation of NCEP sea ice could be avoided. ERA40 and NCEP sea ice cover match quite well (see Section 4.1). The performance of

this simulation was part of the collaboration between BSH and CSC. We used the model version “REMO2009” with slightly adjusted parameters (Dmitry Sein, personal communication).

MPI-253 (1948-2007):

Simulation by REMO coupled with MPIOM. In addition, the model is also coupled with the MPI-M Hydrological Discharge (HD) model (Tomassini and Elizalde, 2012). Outside of the REMO domain, MPIOM is forced by the NCEP atmosphere. REMO is forced by NCEP on the lateral boundaries, too.

IfM-201 (1985-1999):

Simulation by REMO coupled with HAMSOM. REMO and HAMSOM are directly coupled on the HAMSOM domain. The boundary forcing on the ocean layers for HAMSOM is taken from the MPIOM output of the MPI-253 simulation. Outside of the HAMSOM domain, the same MPIOM sea surface output of MPI-253 is taken as lower boundary condition for REMO. The atmospheric lateral boundary conditions from REMO are taken from NCEP. Because of the large SST cold bias of the MPI-253 simulation, it was decided in agreement with BSH that this simulation should be performed in a decade where this SST bias is relatively small.

IfM-123 (1986-1999):

Uncoupled REMO simulation forced by NCEP atmosphere at the lateral boundaries. The lower boundaries at the sea surface are taken from the output of the simulation MPI-253. This simulation is expected to give a similar result as MPI-253, but not exactly the same since the SST forcing is read in 6-hourly, while in the coupled simulation it is updated every coupling time step. Differences to MPI-253 can be attributed to internal variability.

The following two simulations do not belong to the ensemble with the above described model setup with NCEP forcing. However, they are included into the evaluation for comparison:

CSC-300 (1958-2000):

Uncoupled REMO simulation forced by ERA40 reanalysis data. This is an older simulation by an older version of REMO, performed within the ENSEMBLES project (see Chapter 5). The ENSEMBLES domain is smaller than the domain shown in Fig. 1, and covers Europe with a horizontal resolution of 0.22°. The simulation was included into the evaluation to estimate the difference between an NCEP driven, and an ERA40 driven REMO simulation.

IfM-002 (1950-2000):

This is the C20 („control“) simulation of an A1B scenario simulation. It is a

downscaling of an ECHAM5/MPIOM scenario simulation with the coupled REMO/HAMSOM system. Except for the ECHAM5 forcing, the model setup is the same as in the simulation Ifm-201. The simulation was included into the evaluation to estimate the difference between an NCEP driven, and an ECHAM5 driven REMO atmosphere and MPIOM ocean. The SST and the cloud cover of this simulation is compared to MPI-253 in Chapter 4. However, other parameters of this simulation will not be shown since its bias is very similar to that of MPI-253.

IfM and MPI delivered the here mentioned simulations to CSC for evaluation. Further, there exist simulations of the ocean models MPIOM (Jungclaus et al., 2006) and HAMSOM (Pohlmann, 2006) alone, without coupling to REMO. They are evaluated by IfM and MPI and thus are not named in this report. For ease of reading, an overview of the above mentioned simulations, including a short description, is given in Table 1.

Table 1: Overview over the simulations evaluated within this report.

Simulation	Short description	Period
CSC-022	Uncoupled REMO with NCEP forcing	1958-2001
MPI-253	REMO coupled with MPIOM, atmospheric forcing by NCEP	1948-2007
IfM-201	REMO coupled with HAMSOM, atmospheric forcing by NCEP, ocean forcing by MPIOM output of MPI-253	1985-1999
IfM-123	Uncoupled REMO, atmospheric forcing by NCEP, ocean forcing by MPIOM output of MPI-253	1986-1999
CSC-300	Uncoupled REMO with ERA40 forcing	1958-2000
IfM-002	REMO coupled by HAMSOM, A1B scenario simulation forced by ECHAM5/MPIOM (C20 period only)	1950-2000

3 Observational datasets

The simulations described in section 2 are validated with four observational and reanalysis datasets. In the following, a description of all datasets which the model simulation are compared with is given:

NCEP (1948-2012):

NCAR reanalysis product

(<http://www.esrl.noaa.gov/psd/data/reanalysis/reanalysis.shtml>). It provides the atmospheric forcing for the REMO simulations analyzed in this report (except CSC-300), and the SST for the simulation CSC-022.

ERA40 (1957-2002):

ECMWF reanalysis product

(<http://www.ecmwf.int/products/data/archive/descriptions/e4/index.html>). It provides the atmospheric forcing for the simulation CSC-300 and the sea ice cover for CSC-022.

HOAPS-3 (1987-2005):

Satellite derived dataset for the ocean only (<http://www.hoaps.zmaw.de/>)

NOCS (1973-2006):

In-situ ship measurements for the ocean only (<http://noc.ac.uk/science-technology/earth-ocean-system/atmosphere-ocean/noc-surface-flux-dataset>)

These datasets provide monthly mean values of a variety of atmospheric climate variables (including sea surface temperature and sea ice cover), which can be used for comparison to the model simulations, and for comparison of the datasets among each other. These variables are, with the abbreviations and units which are used in the following:

- **TEMP**: Air temperature in 2m height [$^{\circ}\text{C}$]
- **PREC**: Total precipitation [mm/d]
- **EVAP**: Total evaporation [mm/d]
- **SLP**: Sea level pressure [hPa]
- **CCOV**: total cloud cover fraction [%]
- **SRADS**: net surface solar radiation [W/m^2]
- **TRADS**: net surface thermal radiation [W/m^2]
- **AHFS**: surface sensible heat flux [W/m^2]

- **AHFL**: surface latent heat flux [W/m^2]
- **DEW**: Dew point temperature in 2m height [$^{\circ}\text{C}$]
- **QVI**: Vertically integrated water vapor in the atmosphere [kg/m^2]
- **SST**: sea surface temperature [$^{\circ}\text{C}$]
- **SICE**: sea ice cover [%]

The list of available and missing variables for each of the observational / reanalysis datasets is given in Table 2.

Table 2: Available datasets. red cross: variable missing

	NCEP	ERA40	HOAPS	NOCS
TEMP	yes	yes	X	yes
PREC	yes	yes	yes	X
EVAP	X	yes	yes	X
SLP	yes	yes	X	yes
CCOV	X	yes	X	yes
SRADS	yes	yes	X	yes
TRADS	yes	yes	yes	yes
AHFS	yes	yes	yes	yes
AHFL	yes	yes	yes	yes
DEW	X	yes	X	yes
QVI	X	X	yes	X
SST	yes	yes	yes	yes
SICE	yes	yes	X	yes

4 Validation of the REMO simulations with observational data

This chapter contains a validation of the REMO simulations with the observational / reanalysis data, including a comparison of the observational data among each other. The boundary conditions of the simulations IfM-201 and IfM-123 are prescribed by the simulation MPI-253 and are thus expected to deviate from it only in the North Sea region. Therefore, only the simulations MPI-253, CSC-022, and CSC-300 are included in the validation, while the comparison of the IfM simulations to the other REMO simulations is given in the next chapter. In the following, an analysis is shown for all variables listed in Table 2. The reference period 1961-2000 is chosen if possible. However, the datasets HOAPS and NOCS do not cover the entire period, such that a shorter time period has to be used for comparison. Here, we choose the period 1987-1999 which is covered by both datasets.

4.1 Sea surface temperature and sea ice cover

The SST of ERA40 is used as reference for horizontal plots (see Fig. 2). The differences between CSC-022 and ERA40 are relatively small over the North Atlantic and the North Sea region, except at the areas with sea ice cover. Note that the SST of CSC-022 is identical to the NCEP-SST, therefore the difference between NCEP and ERA40 SST is identical. In the period 1987-1999, the reanalysis datasets agree well with NOCS, while HOAPS is slightly lower over the North Atlantic. Differences near the ice sheets are probably caused by the artifact that regions which are partly covered by sea ice in winter (< 50% in the yearly mean) are not masked out, and might thus contain unrealistic values.

The largest SST differences to ERA40 are seen for the simulation MPI-253. This simulation has a cold bias of over 2 °C over the GIN sea, and between 1 and 2 °C over the North Sea and Baltic Sea. In the region near the South-Eastern coast of Greenland, close to the western boundary of the domain, a warm bias of up to 2 °C is seen, however this region is probably too far away to affect the SST in the North Sea region, which is much stronger affected by the SST and the sea ice over in the GIN sea. A very similar behavior is shown by the ECHAM5/MPIOM driven simulation IfM-002, indicating that this bias is probably caused by problems with the REMO/MPIOM coupling. For new test simulations with MPI-ESM forcing for RCP scenarios, REMO and MPIOM have been tuned to give improved results (Dmitry Sein, personal communication). Wind stress might also play a role: Not enough sea ice is transported out of the GIN sea, leading to the cold bias in this region. This has now also been improved.

On the coupling of the oceanic North Sea model HAMSOM with the regional atmospheric model REMO

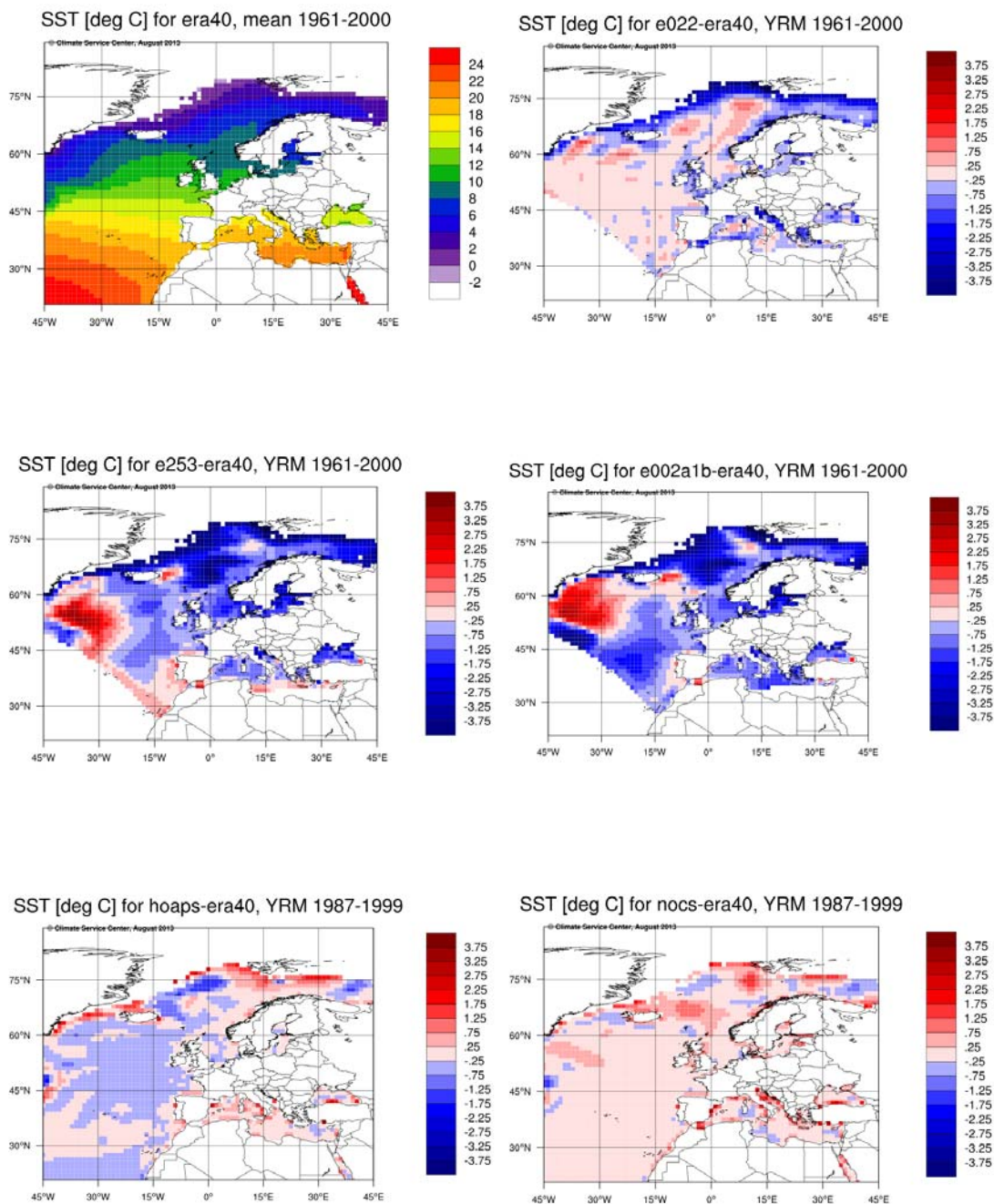


Figure 2: Top left: Mean SST [°C] of ERA40 for the period 1961-2000. Top right: SST difference of CSC-022 to ERA40. Middle: SST difference of MPI-253 (left) and IfM-002 (right) to ERA40. Bottom left: SST difference of HOAPS (left) and NOCS (right) to ERA40 in the period 1987-1999. Regions with more than 50% mean sea ice cover are masked out.

The time development of the mean averaged SST over the North Sea has been analyzed by BSH (see Fig. 3). In contrast to MPI-253, an uncoupled MPIOM simulation, driven by NCEP, follows the observation closely with a slight warm bias, strengthening the notion that the cold bias is caused the REMO/MPIOM coupling.

The cold bias is most severe in the 1970s and 1980s, while it is smaller in the period 1985 to 2000. Therefore, it was decided to use this period for the REMO/HAMSOM hindcast simulation IfM-201.

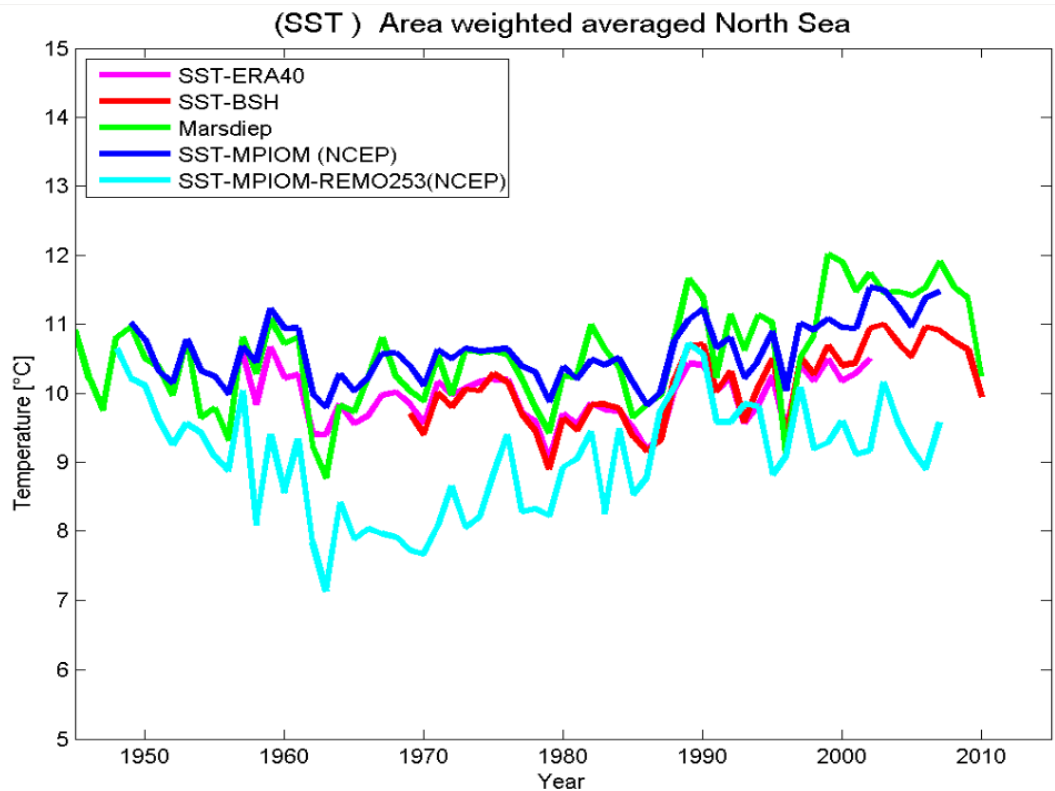


Figure 3: Time development of area averaged SST over the North Sea for ERA40 (pink), BSH observational dataset (red), Marsdiep *in situ* measurement (green), simulation with NCEP driven uncoupled MPIOM (blue), simulation MPI-253 (turquoise). Figure provided by BSH.

The yearly mean sea ice concentration of ERA40, as well as the differences to NCEP, NOCS, and the simulation MPI-253, are shown in Figure 4. Note that the sea ice cover of simulation CSC-022 is prescribed by NCEP, therefore it does not have to be shown. The difference plots show that NCEP and ERA40 sea ice concentration are very similar, while the simulation MPI-253 has a higher sea ice concentration, which is consistent with the lower SST in the GIN sea. However, NOCS also shows higher sea ice concentration than ERA40 and therefore its sea ice cover is close that if MPI-253, although its SST is higher.

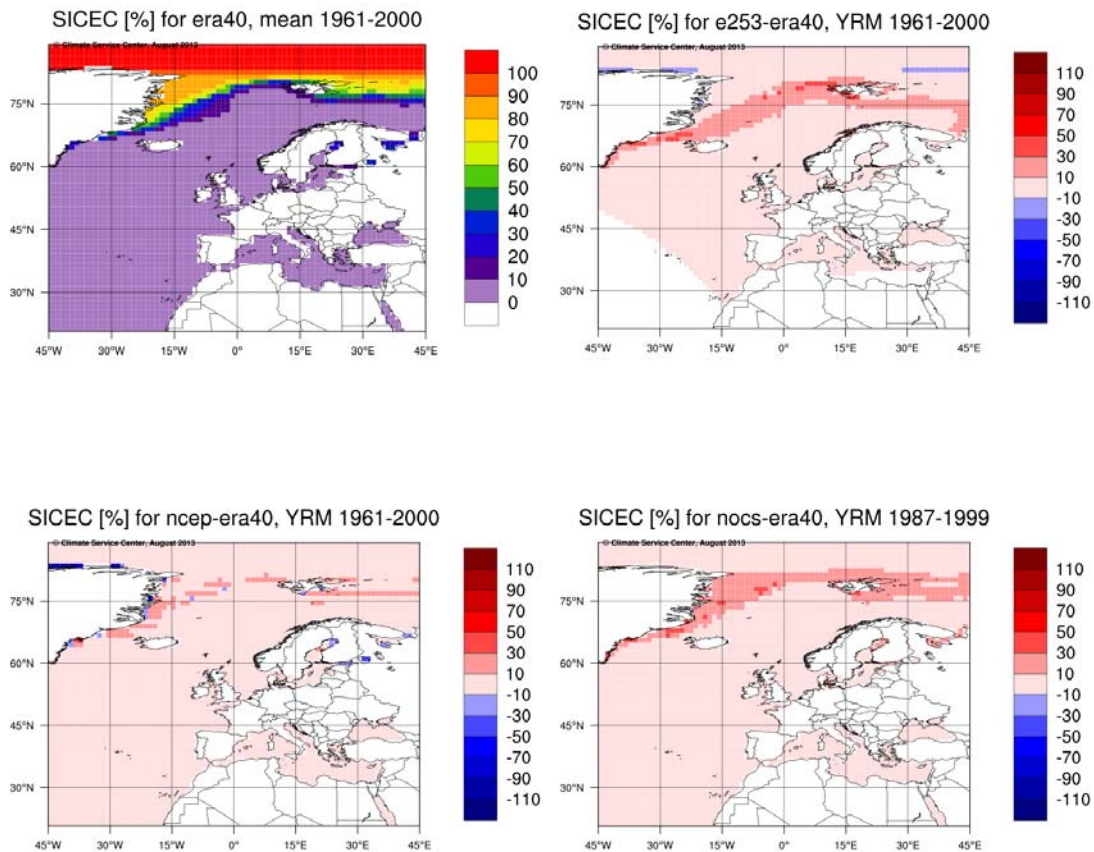


Figure 4: Top left: Sea ice cover of ERA40 [%]. Top right: Difference in sea ice cover between simulation MPI-253 to ERA40. Bottom: Difference in sea ice cover between NCEP (left) and NOCS (right) to ERA40. In the difference plots, positive values indicate higher mean sea ice concentration than the reference simulation (ERA40).

4.2 Near surface air temperature

Differences of 2m temperature to ERA40 reanalysis data are shown in Fig. 5. There are differences in temperature between NCEP and ERA40, especially over land: Here, NCEP is cooler in general, especially in winter (up to 2 °C), where it is also strongly colder over the ice sheets. Over the GIN sea and near the European coast lines, NCEP tends to be slightly warmer than ERA40 in winter. Over the ocean NOCS temperatures are slightly warmer than ERA40 in winter and slightly cooler in summer in the period 1986-1999 (not shown).

On the coupling of the oceanic North Sea model HAMSOM with the regional atmospheric model REMO

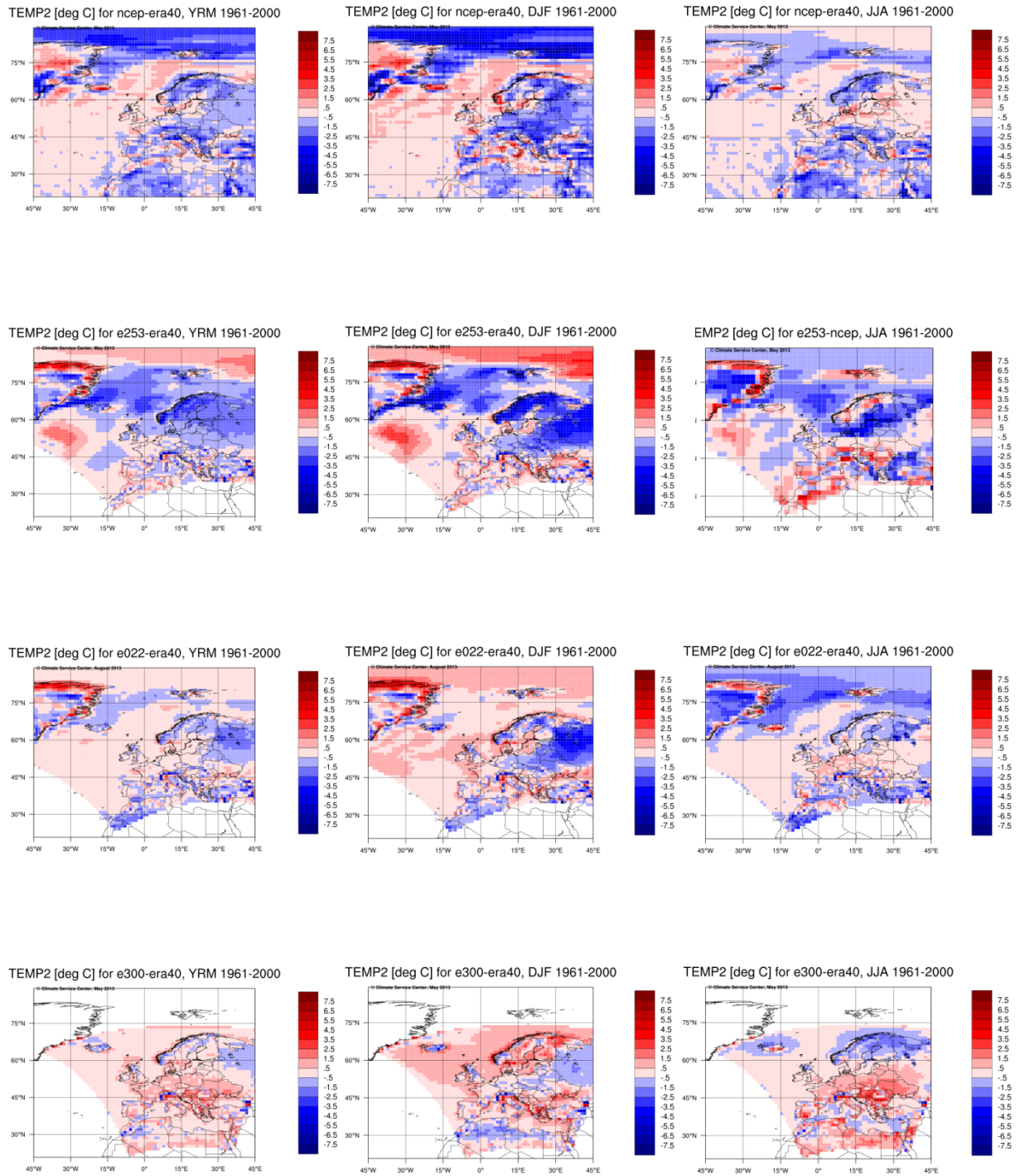


Figure 5: Differences in 2m temperature to ERA40 [°C] for the period 1961-2000. Rows from top to down: NCEP, MPI-253, CSC-022, CSC-300. Columns from left to right: yearly mean, winter (DJF) mean, summer (JJA) mean.

Over the ocean, the 2m temperatures of the simulations follow the SST closely and show very similar biases, as can e. g. be seen from the bias of the NCEP-SST driven CSC-022 simulation, which is similar to the difference between NCEP and ERA40. However, different biases can be seen over land, where CSC-022 temperatures are similar to ERA40 in Central- and Western Europe, while there is a strong cold bias in North-Eastern Europe in winter. This means, REMO tends to increase the NCEP temperatures over Europe, except in North-Eastern Europe in winter. This is consistent with the ERA40 driven CSC-300 simulation, which tends to be warmer than ERA40 over Europe except in North Eastern Europe. However, the cold bias, which CSC-300 shows over Scandinavia in summer seems to be improved in the CSC-022 simulation. This might be due to the improved REMO model version which was used for CSC-022.

The temperature bias of MPI-253 closely follows its SST bias over the ocean. Even if the temperature of MPI-253 over land is slightly smaller than CSC-022, it seems that the SST cold bias does not affect the land temperatures too much, such that the bias patterns of both simulations look rather similar, although MPI-253 has a stronger cold bias over Scandinavia.

4.3 Precipitation

ERA40 absolute precipitation as well as the differences of NCEP, HOAPS, MPI-253, CSC-022, and CSC-300 precipitation to ERA40 are presented in Fig. 6. The REMO simulations generally tend to have more precipitation than ERA40, both over ocean and over land. This is seen in all seasons, however, the differences are strongest in winter and weaker in summer. The differences between the simulations MPI-253 and CSC-022 are very small, except in winter over the North Atlantic region south of Greenland where MPI-253 shows the strong SST warm bias. This observation indicates that REMO precipitation over Europe and regions near to the European coasts, including the North Sea region, is dominated by the atmospheric part of the simulation, while the different SST of the MPI-253 simulation has only a minor effect. Actually the differences between the coupled MPI-253 and uncoupled CSC-022 simulations are smaller than the differences between the uncoupled simulations CSC-300 and CSC-022 which are run by different REMO versions. The bias of the scenario simulation IfM-002 is also close to that of MPI-253 (not shown).

There are also differences between the observational datasets: NCEP is drier than ERA40, and therefore even farther away from the precipitation simulated by REMO, while the precipitation provided by the HOAPS dataset is close to ERA40.

On the coupling of the oceanic North Sea model HAMSOM with the regional atmospheric model REMO

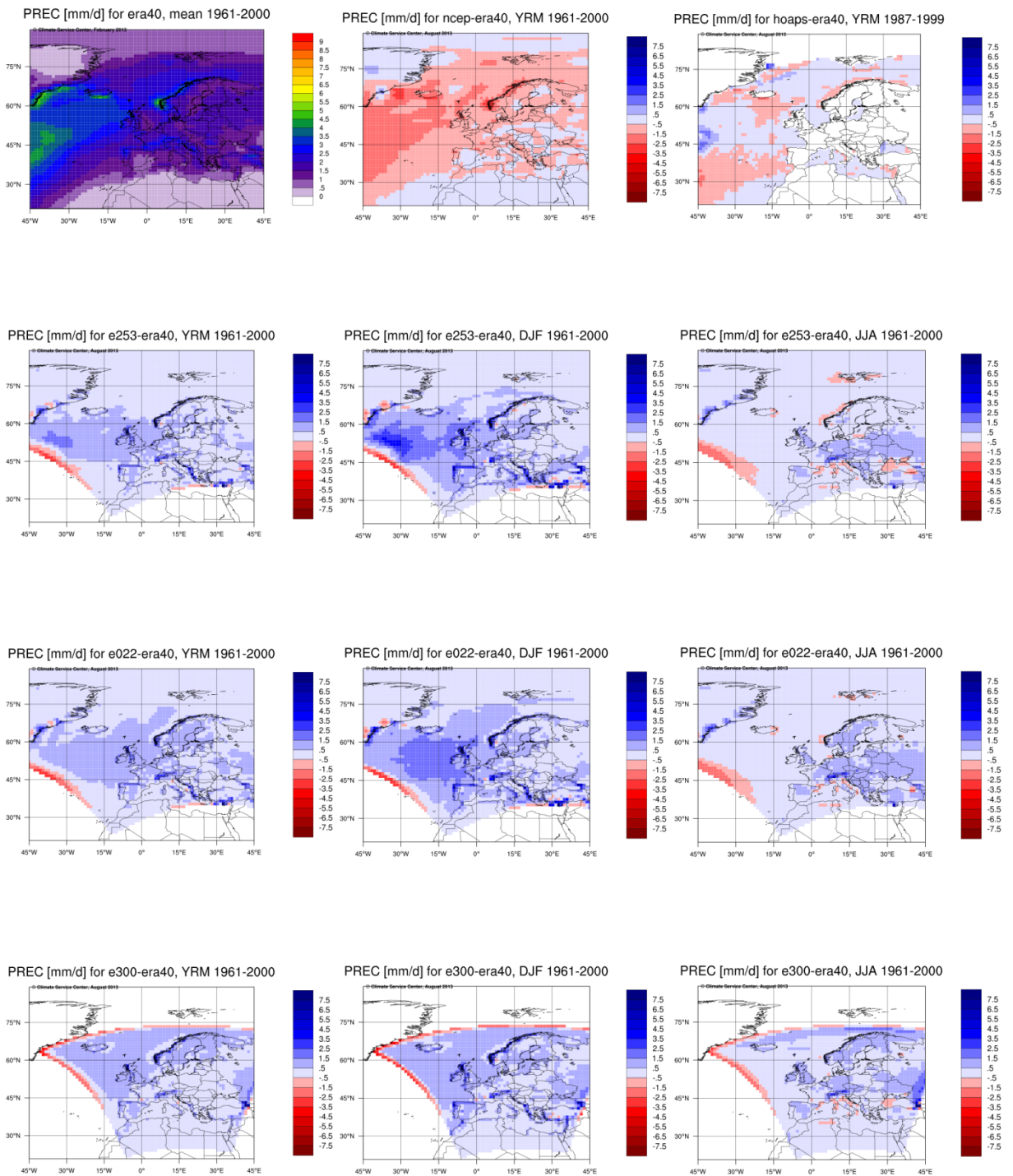


Figure 6: Top row from left to right: Yearly mean precipitation [mm/d] of ERA40 (1961-2000), and difference of NCEP (1961-2000), and HOAPS (1987-1999) to ERA40. Row 2-4: Difference in precipitation of REMO simulations MPI-253, CSC-022, and CSC-300 to ERA40 (1961-2000), yearly mean (left column), DJF (middle column), JJA (right column).

4.4 Evaporation

Absolute differences in evaporation of the three simulations MPI-253, CSC-022, and CSC-300 (for the period 1961-2000), and HOAPS (ocean only, 1986-1999) to ERA40 is shown in Fig. 7. All REMO simulations show the common feature that in winter there is more evaporation than ERA40 over the ocean, while there is less over land. In summer the opposite observation is made, with less evaporation over the ocean and more over land. This feature is weakest for the CSC-300 simulation, probably due to the fact that it is driven by ERA40, and is therefore closer to the forcing dataset. The strongest differences to ERA40 are shown by the coupled simulation MPI-253 over the ocean, probably caused by the SST cold bias. However, in contrast to the uncoupled REMO simulations, MPI-253 shows less evaporation over the GIN sea where it has the strongest SST cold bias, even in winter. Further, MPI-253 shows a strong low-evaporation bias in summer over the North Sea. In the region south of Greenland where MPI-253 has a warm bias, a strong increase in evaporation is seen in winter.

A comparison of ERA40 with HOAPS shows, that there is a similar behavior of HOAPS compared to the REMO simulations, with more evaporation over the ocean in winter, and less in summer. This indicates that the REMO evaporation is closer to HOAPS and the evaporation provided by ERA40 might have a problem, as it is also observed in the latent heat flux (see section 4.7). However, in the yearly mean, HOAPS has less evaporation over ocean than ERA40, while the REMO simulations tend to have more.

On the coupling of the oceanic North Sea model HAMSOM with the regional atmospheric model REMO

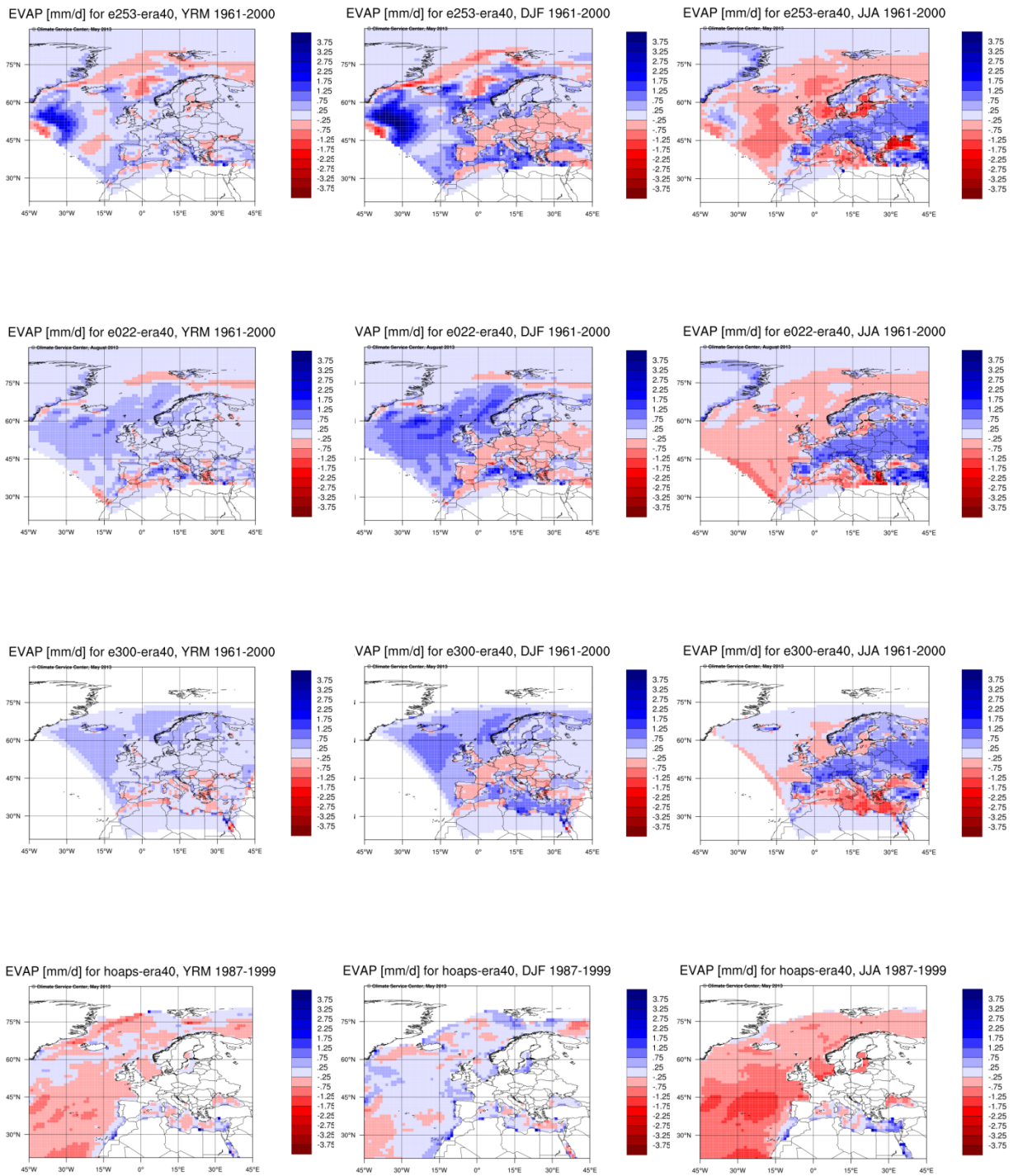


Figure 7: Differences in evaporation to ERA40 [mm/d] for the period 1961-2000. Rows from top to down: MPI-253 (1961-2000), CSC-022 (1961-2000), CSC-300 (1961-2000), HOAPS (1987-1999). Columns from left to right: yearly mean, winter (DJF) mean, summer (JJA) mean.

4.5 Cloud cover

ERA40 cloud cover as well as the differences of the coupled (MPI-253, IfM-002) and uncoupled (CSC-022, CSC-300) REMO simulations are shown in Fig. 8, for the time period 1961-2000. The difference of the NOCS dataset to ERA40 is also shown for the period 1986-1999. A common feature of all REMO simulations is, that they have more cloud cover than ERA40 over the ocean (except for the Arctic region around Spitsbergen), but less over Europe (except an area near to the Baltic Sea coast in Sweden and Finland). This is the case for all seasons (not shown). Although the differences between the REMO simulations are very small, the bias with respect to ERA40 is slightly lower in the North Sea region for the uncoupled CSC-022 simulation than for the three other simulations. This might be due to the tuning of the REMO version with which CSC-022 was simulated.

Similar as for the evaporation, the differences between NOCS and ERA40 cloud cover look similar to the REMO simulations, with more cloud cover over the ocean, and less over the Arctic, meaning that REMO cloud cover is closer to NOCS than to ERA40.

On the coupling of the oceanic North Sea model HAMSOM with the regional atmospheric model REMO

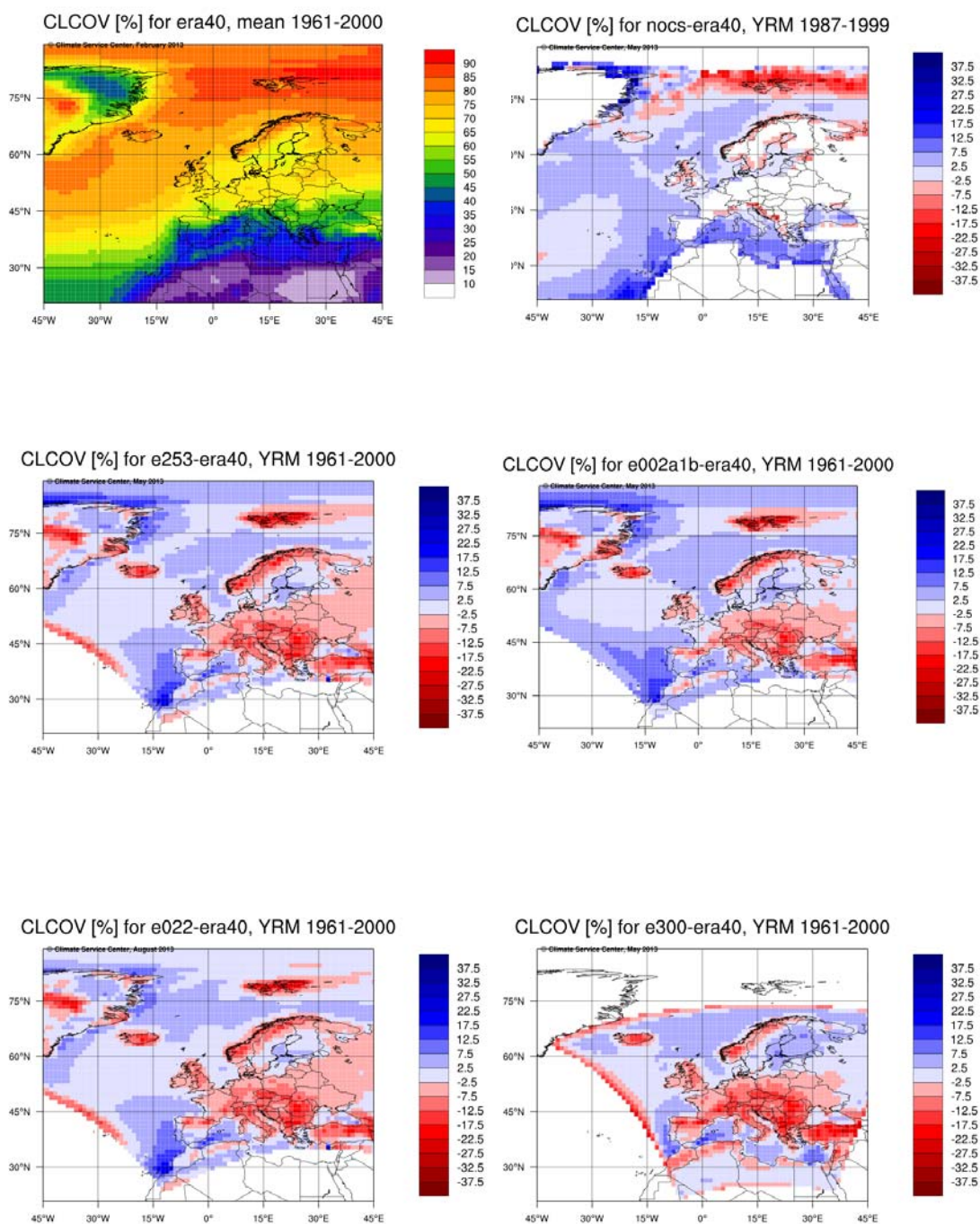


Figure 8: Top left: Cloud cover fraction [%] of ERA40 dataset, mean 1961-2000. Top right: Difference of NOCS and ERA40 cloud cover (ocean only), mean over 1986-1999. Middle left to bottom right: Difference in cloud cover of REMO simulations MPI-253, IFM-002, CSC-022, and CSC-300 to ERA40, mean over 1961-2000.

4.6 Sea level pressure

ERA40 mean sea level pressure as well as the differences of NCEP, NOCS, MPI-253, CSC-022, and CSC-300 mean sea level pressure to ERA40 are shown in Fig. 9. The NCEP dataset has a higher mean sea level pressure than ERA40 over Greenland, and a lower one over the Arctic, while both datasets agree well in the largest part of the domain. The large difference over Greenland may be due to the fact that the SLP in ERA40 has been extrapolated to sea level from high altitudes, such that ERA40 might not be reliable in this region. The sea level pressure of NOCS is higher than ERA40, especially over the GIN sea and near the East coast of Greenland.

The REMO simulations show generally lower sea level pressure values, especially over Europe. The difference to ERA40 is particularly strong in winter. While the difference pattern for the NCEP driven coupled MPI-253 and the uncoupled CSC-022 look very similar, in all seasons, there are differences to the CSC-300 simulation. In winter, the strong low pressure anomaly over Europe of CSC-300 is smaller in extent. In summer, CSC-300 shows a relatively homogeneous low pressure bias (except over North Africa), while both NCEP forced simulations have high pressure anomalies over Scandinavia, Iceland, and the Mediterranean. Throughout the year, the MPI-253 and CSC-022 also show a strong high pressure anomaly over Greenland and thus follow their NCEP forcing dataset. This area is out of the ENSEMBLES domain of CSC-300.

The fact that the sea level pressure anomalies of MPI-253 and CSC-022 are very similar despite their large SST differences, indicates that the pressure patterns are mainly generated by the atmospheric forcing of the REMO model, and are not strongly affected by the SST bias generated by the REMO/MPIOM coupling. However, the MPI-253 SLP bias shows a lower gradient north of the North Sea than CSC-022 in winter, indicating a difference in the dynamics. The different behavior of the CSC-300 simulation is probably caused by the different forcing dataset (ERA40) and the different domain size.

On the coupling of the oceanic North Sea model HAMSOM with the regional atmospheric model REMO

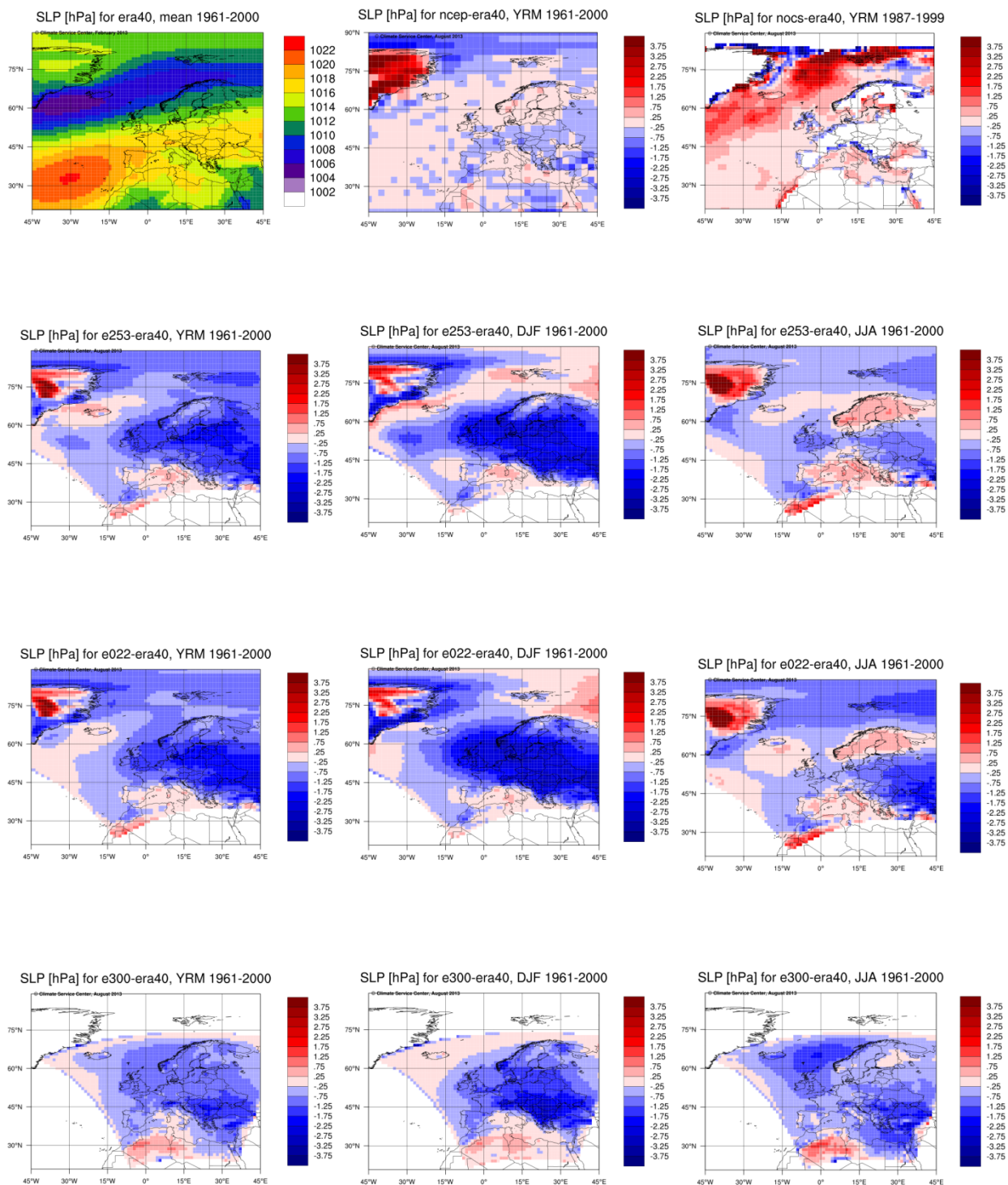


Figure 9: Top row from left to right: Yearly mean sea level pressure [hPa] of ERA40 (1961-2000), and difference of NCEP (1961-2000), and NOCS (1987-1999). Row 2-4: Difference in mean sea level pressure of REMO simulations MPI-253, CSC-022, and CSC-300 to ERA40 (1961-2000), yearly mean (left column), DJF (middle column), JJA (right column).

4.7 Surface fluxes

For the latent and sensible heat fluxes, datasets are available for all four reanalysis and observational datasets. While NCEP, HOAPS, and NOCS agree largely over the ocean, the ERA40 heat fluxes show large seasonal differences to the three other datasets (not shown). Therefore it is assumed that the seasonal variation of ERA40 heat fluxes might be problematic, and therefore NCEP is chosen as reference dataset. NCEP mean latent and sensible heat fluxes, and the differences of HOAPS and NOCS, MPI-253, CSC-022, and CSC-300 heat fluxes to NCEP are shown in Figs. 10 and 11, respectively. The differences between both HOAPS and NOCS to NCEP over the ocean are slightly positive (i.e. less heat flux from the surface to the atmosphere). This is the case for all seasons, except for NOCS in summer where there is a good agreement with NCEP (not shown).

All REMO simulations have in common that there is a positive bias (i.e. less heat flux) in the *latent* heat flux over land in all seasons compared to NCEP. In winter, the bias is negative for the uncoupled simulations CSC-022 and CSC-300 over the ocean, but MPI-253 has a positive anomaly in the GIN sea, probably due to the SST cold bias. In summer, CSC-022 and CSC-300 are rather similar over the North Sea and the GIN seas, while the positive anomaly of MPI-253 is prevalent. Over the continent, *sensible* heat flux shows a negative bias (i.e. more heat flux from surface to atmosphere) in winter (especially in Eastern Europe) but a positive bias in summer. Over the ocean, there is a slight positive anomaly in winter, which is larger in MPI-253 in a small domain in the GIN Sea.

On the coupling of the oceanic North Sea model HAMSOM with the regional atmospheric model REMO

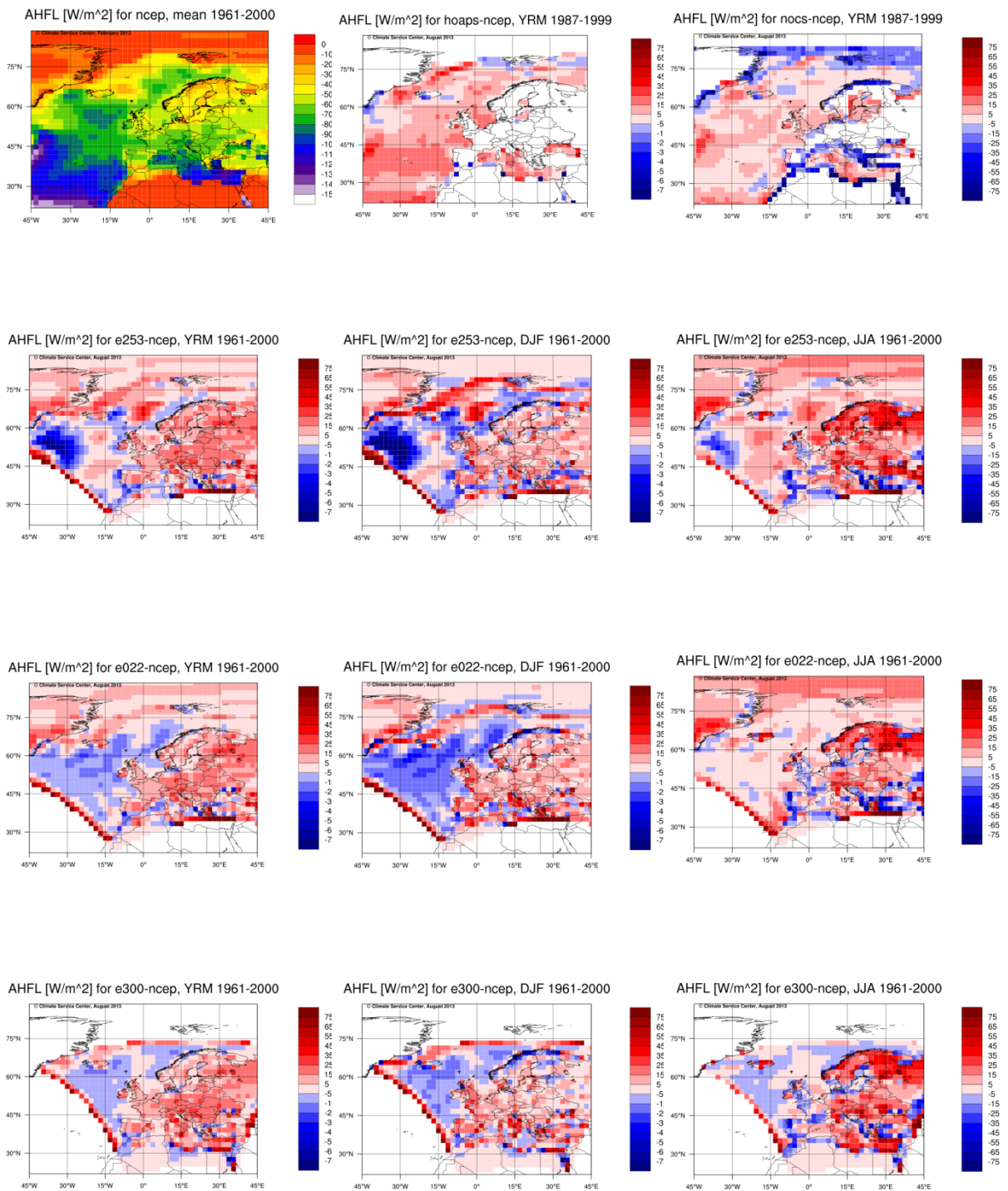


Figure 10: Top row from left to right: Yearly mean latent heat flux [W/m²] of NCEP (1961-2000), and difference of HOAPS and NOCS (1987-1999) to NCEP. Row 2-4: Difference in mean latent heat flux of REMO simulations MPI-253, CSC-022, and CSC-300 to NCEP (1961-2000), yearly mean (left column), DJF (middle column), JJA (right column). Note that AHFL is negative, i.e. in the difference plots, negative values (blue colors) indicate higher latent heat flux.

On the coupling of the oceanic North Sea model HAMSOM with the regional atmospheric model REMO

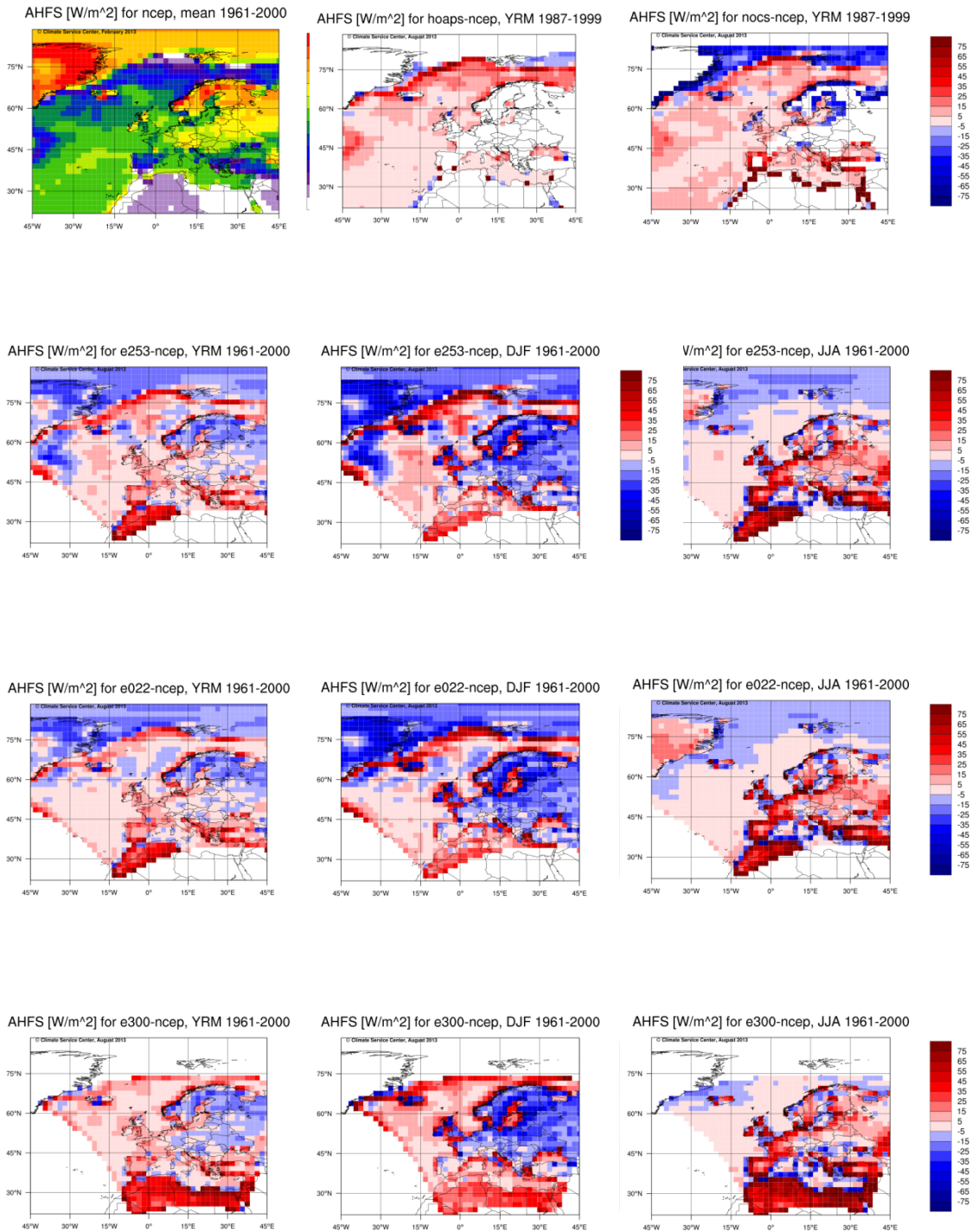


Figure 11: Top row from left to right: Yearly mean sensible heat flux [W/m²] of NCEP (1961-2000), and difference of HOAPS and NOCS (1987-1999) to NCEP. Row 2-4: Difference in mean sensible heat flux of REMO simulations MPI-253, CSC-022, and CSC-300 to NCEP (1961-2000), yearly mean (left column), DJF (middle column), JJA (right column). Note that positive values of AHFS indicate heat transported from the atmosphere to the surface, and vice versa.

4.8 Radiation

Similar as for the surface fluxes, there are large seasonal differences between ERA40 and NCEP net solar and net thermal radiation at the surface (not shown). Net radiation is also available for the NOCS dataset, which is closer to NCEP than to ERA40 in the case of solar radiation, leading to the assumption that the NCEP net solar radiation is better. On the other hand, the thermal radiation of NOCS is closer to ERA40. To be consistent with the surface fluxes presented in section 4.7, we propose to use the NCEP dataset as reference for the radiation, too.

Figs. 12 and 13 show the differences of the observational datasets and the model simulation MPI-253, CSC-022, and CSC-200 to NCEP net solar / thermal radiation. As stated above, the differences between NCEP and ERA40 are large: In the yearly mean, ERA40 has less solar and thermal radiation. However, there are also differences between NOCS and NCEP (less solar radiation north of ca. 45°N, less thermal radiation in the whole domain). On the other hand, HOAPS shows more thermal radiation (solar radiation not available). Overall, there are large differences in the observational datasets. However, all REMO simulations show systematically less net solar and thermal radiation at the surface, compared to NCEP. This picture is seen throughout the year in all seasons. The systematically low radiation values are a known feature of REMO, however the radiation bias is of the same order as the disagreement of the observational data.

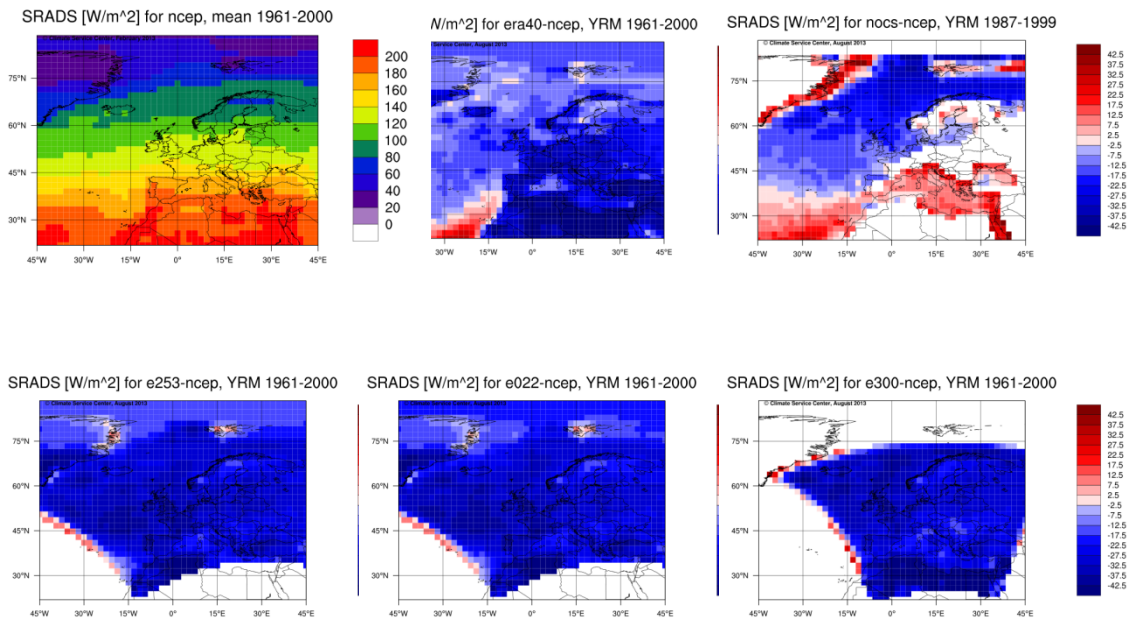


Figure 12: Top row (left to right): Yearly mean net surface solar radiation [W/m²] of NCEP (1961-2000), and difference of ERA40 (1961-2000) and NOCS (1987-1999) to NCEP. Bottom: Difference in yearly mean solar radiation of REMO simulations MPI-253, CSC-022, and CSC-300 to NCEP (1961-2000).

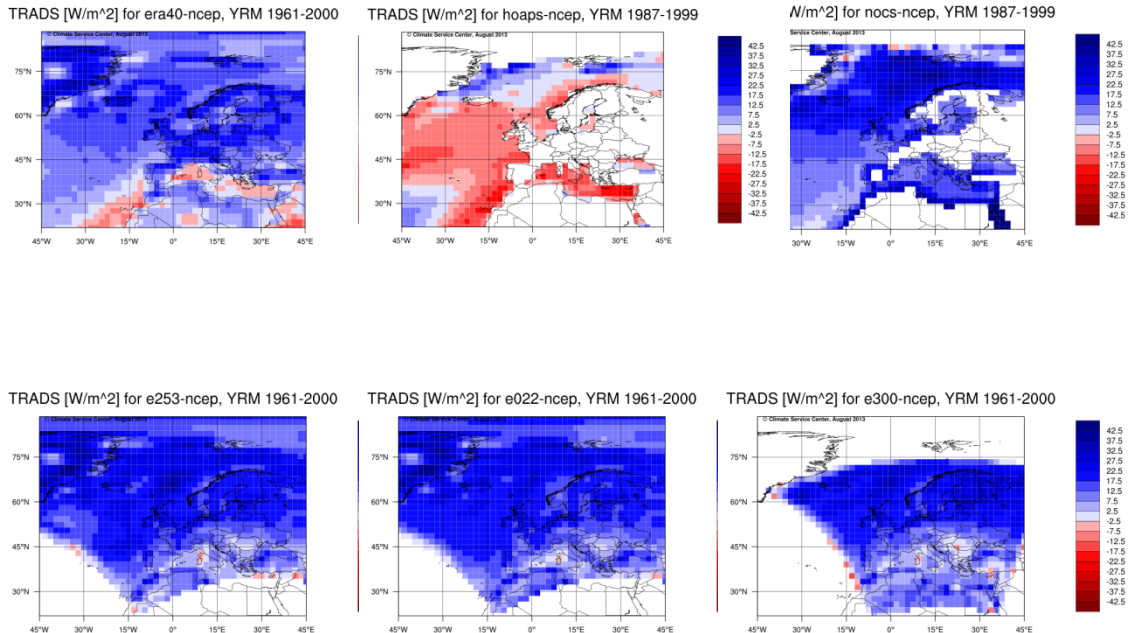


Figure 13: Top row: Difference in yearly mean net surface thermal radiation [W/m²] of ERA40 (1961-2000), HOAPS, and NOCS (1987-1999) to NCEP. Bottom row: Difference in yearly mean net surface thermal radiation of REMO simulations MPI-253, CSC-022, and CSC-300 to NCEP (1961-2000). Note that positive values indicate less thermal radiation.

5 Estimation of the REMO simulations within the bandwidth of the ENSEMBLES regional model simulations

The ENSEMBLES project provides an ensemble of 16 ERA40 driven regional climate model simulations for Europe on a horizontal resolution of 25 km (van der Linden and Mitchell, 2009, Jacob et al., 2012). These simulations have been used to estimate how the REMO simulations MPI-253 and CSC-022 are located within the bandwidth, which is spanned by the ensemble. Monthly mean values of TEMP2, DEW2, PREC, EVAP, CCOV, SLP, AHFL, AHFS, SRADS, and TRADS have been downloaded¹ and averaged over four regions within the North Sea. The region masks have been designed to fit those, which are used by BSH (Bülow et al., 2013), see Fig. 14. The mean values of each ENSEMBLES simulation are built and the set of all values are presented as a so-called “box-whisker” plot. They consist of a “box”, showing the inner-quartile of the distribution (the median is marked with a horizontal line within the box), and the “whiskers”, which are extended until the minimum or, respectively, the maximum value, but not more than 1.5 times the inner-quartile range. Values, which are beyond this range, are marked as “outliers”. The mean value, including all outliers, is marked by a fat dot. All ENSEMBLES simulations are “anonymous” within the box-whisker plots. Some variables are missing for some of the simulations, such that for those variables the value distribution consists of less than 16 members. Note that the CSC-300 simulation is one of the ensemble members.

1 The data have been download from <http://ensemblesrt3.dmi.dk/data/ERA40/>

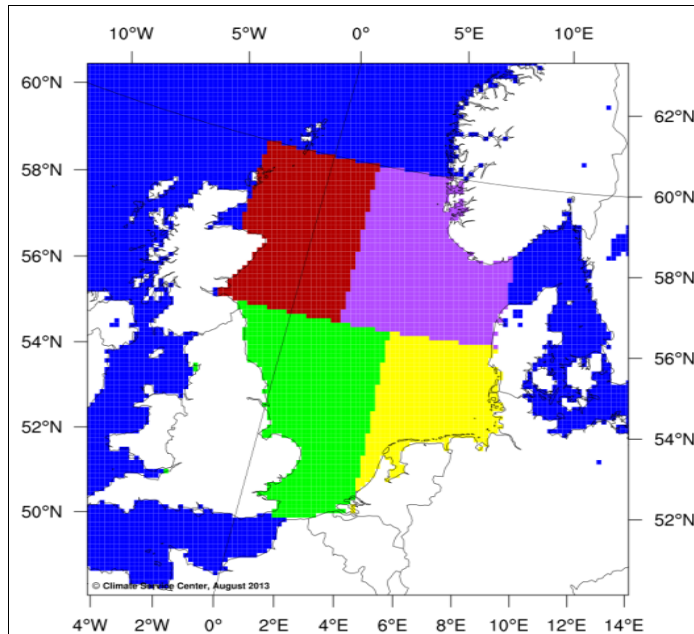


Figure 14: Map of the four domains of the North Sea, used for averaging: Red: North west (NW), purple: north east (NE), green: south west (SW), yellow: south east (SE).

Within each box-whisker plot, the respective values of the coupled MPI-253 simulation, and of the uncoupled CSC-022 simulation are plotted. This allows estimating if the two REMO simulations are close to the median of the ensemble within the North Sea region, or if they are more shifted toward the tail of the distribution, or if they should be considered as outliers. In the following, we describe the results for the different quantities, and assess them with respect to the validation given in Chapter 3:

- **2m temperature** (Fig. 15): The simulation MPI-253 is clearly colder than the ensemble in all seasons and can be considered as an outlier, except for the autumn where it reaches temperatures which are close to the lower end bandwidth. The reason is probably the SST cold bias of the MPI-253 simulation as described in Section 4.1. In contrast, the temperature ranges of the uncoupled CSC-022 simulation are placed well in the center of the ensemble.
- **2m dew point temperature** (Fig. 16): The dew point temperature in combination with the temperature determines the relative humidity. However, if as in the present case only monthly mean values are available, only a rough estimate of the qualitative behavior of the relative humidity is possible. While CSC-022 temperatures are in the center of the ensemble, its dew point temperature is on the lower end of the bandwidth, except in summer. This indicates that the CSC-022 simulation has a lower surface-near relative humidity than the bulk of the ENSEMBLES simulations in autumn, winter, and spring.

- **Precipitation** (Fig. 17): The mean precipitation amount of MPI-253 and CSC-022 are very similar at all seasons and all four subregions of the North Sea. This confirms the general observation stated in Section 4.3, that the precipitation difference of all REMO simulations is very small. In fact, the plots shows that it is considerably smaller than the bandwidth of the ENSEMBLES simulations. The seasonal precipitation sums are at the high end of the bandwidth in autumn and winter, while they are in the center in spring and summer.
- **Evaporation** (Fig. 18): REMO evaporation is at the upper end of the bandwidth in autumn, and in the Northern areas also in winter. CSC-022 has slightly higher evaporation than MPI-253 in autumn, winter, and spring. However, this difference is very large in summer, where CSC-022 is in the center of the ensemble, while MPI-253 is a clear outlier on the low-evaporation edge, especially in the North-Eastern region. This confirms the observation of a strong low-evaporation bias of MPI-253 in the North Sea in summer. It is probably caused by the SST cold bias. Both simulations are close to the center of the ensemble in spring.
- **Cloud cover fraction** (Fig. 19): The bandwidth of the ENSEMBLES simulations is clearly larger than the differences between both REMO simulations. This is in line with the observation stated in section 4.5, that the differences between the observational datasets in cloud cover are larger than the differences of the REMO simulations among each other. The REMO mean cloud cover lies well inside the inner-quartile range of the ensemble for all seasons and regions in the North Sea.
- **Sea level pressure** (Fig. 20): The mean sea level pressure of both REMO simulations over the North Sea is located clearly on the low-pressure outliers side. This is the case on all seasons, only in summer it is less severe but still on the low end of the band width. This is consistent with the low pressure bias of CSC-022 and MPI-253 relative to ERA40, NCEP, and NOCS (see Section 4.6).
- **Surface heat fluxes** (Figs. 21 and 22): The SST cold bias of MPI-253 induces reduced heat fluxes with respect to CSC-022 over the North Sea, especially in summer and autumn. The latent heat flux of CSC-022 lies on the negative (i.e. too high heat flux) outliers end of the ensemble in autumn, in the Northern areas also in winter. These are the same areas where the CSC-022 evaporation is also higher. On the other hand, sensible heat flux lies within the center of the ensemble distribution for all seasons and subregions. The reduced heat fluxes of MPI-253 lead to compensation of the high latent heat fluxes of CSC-022 in autumn and winter, but to a shift to the positive (too low heat flux) outliers side in summer. A too low sensible heat flux of MPI-253 with respect to the ENSEMBLES simulations is only seen in summer in the North Eastern

subregion.

- **Net surface radiation** (Figs. 23 and 24): In Section 4.8, a deficit in surface radiation of the REMO simulations was found by comparison with the observations, visible as a negative bias in net solar-, and a positive bias in net thermal radiation. The comparison with the ENSEMBLES simulations over the North Sea shows consistently, that the net surface solar radiation of MPI-253 and CSC-022 lies below the mean and median, and the thermal radiation lies above. However, the spread within the radiation values provided by ENSEMBLES is large, such that the two REMO simulations generally lie within the inner-quartile range of the distribution and are therefore not on the outliers side. A deviation of MPI-253 to CSC-022 is only seen in summer (all subregions), with a reduced thermal radiation leading to a positive anomaly.

On the coupling
of the oceanic
North Sea model
HAMSOM with
the regional
atmospheric
model REMO

On the coupling of the oceanic North Sea model HAMSOM with the regional atmospheric model REMO

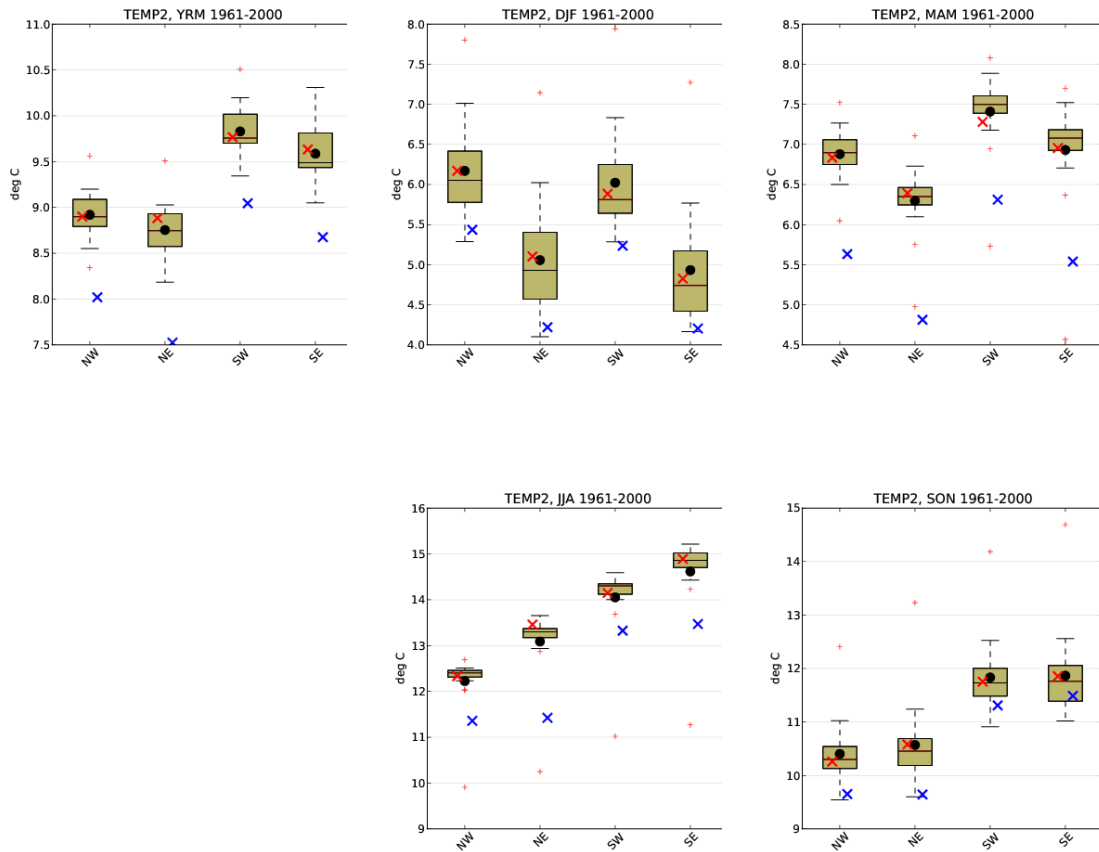


Figure 15: The box-and-whisker show the bandwidth of the ENSMBLES hindcast simulations for the 2m air temperature [$^{\circ}\text{C}$], averaged over the period 1961-2000 and over the four domains of the North Sea NW, NE, SW, SE as shown in Fig. 14. The vertical black line within each box denotes the median value, while the mean value is marked by a black dot. Small red “+” symbols are outliers. Large crosses indicate the position of the CSC-022 simulation (red), and the MPI-253 simulation (blue). Top row from left to right: Yearly mean (YRM), winter (DJF), spring (MAM); bottom row: summer (JJA), autumn (SON).

On the coupling of the oceanic North Sea model HAMSOM with the regional atmospheric model REMO

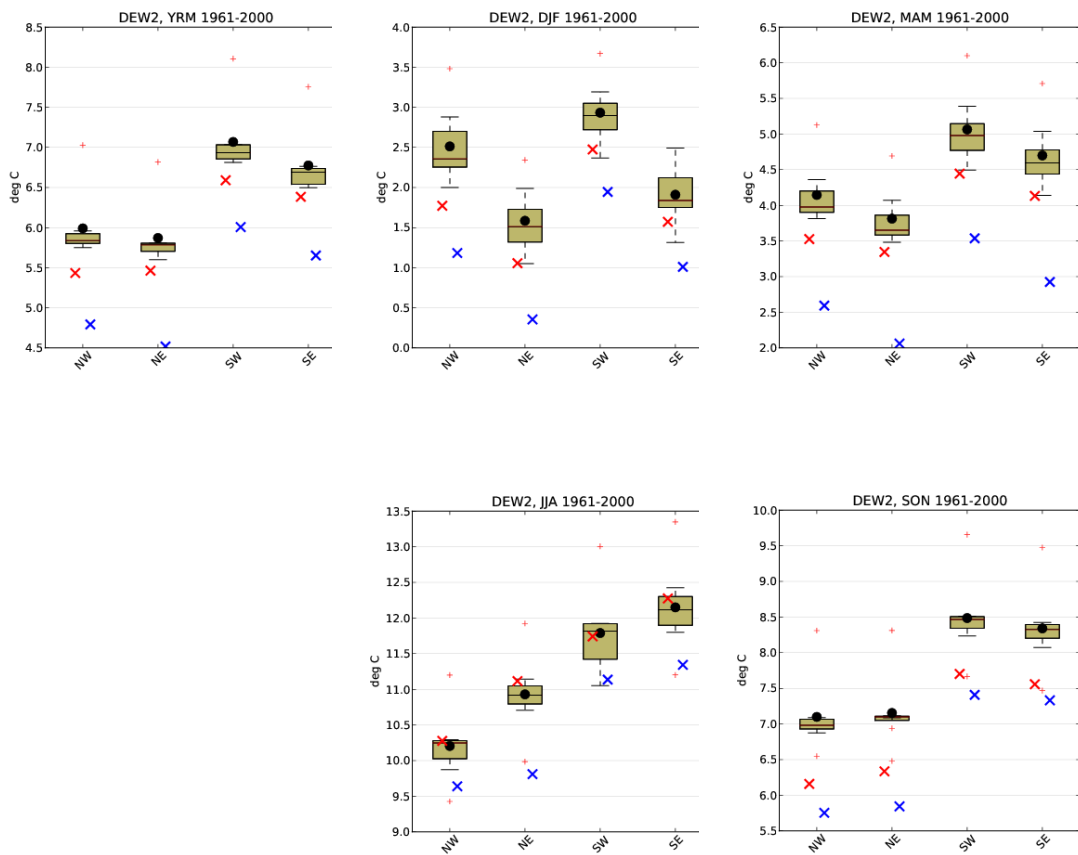


Figure 16: Similar as Fig. 15, for 2m dew point temperature [°C].

On the coupling of the oceanic North Sea model HAMSOM with the regional atmospheric model REMO

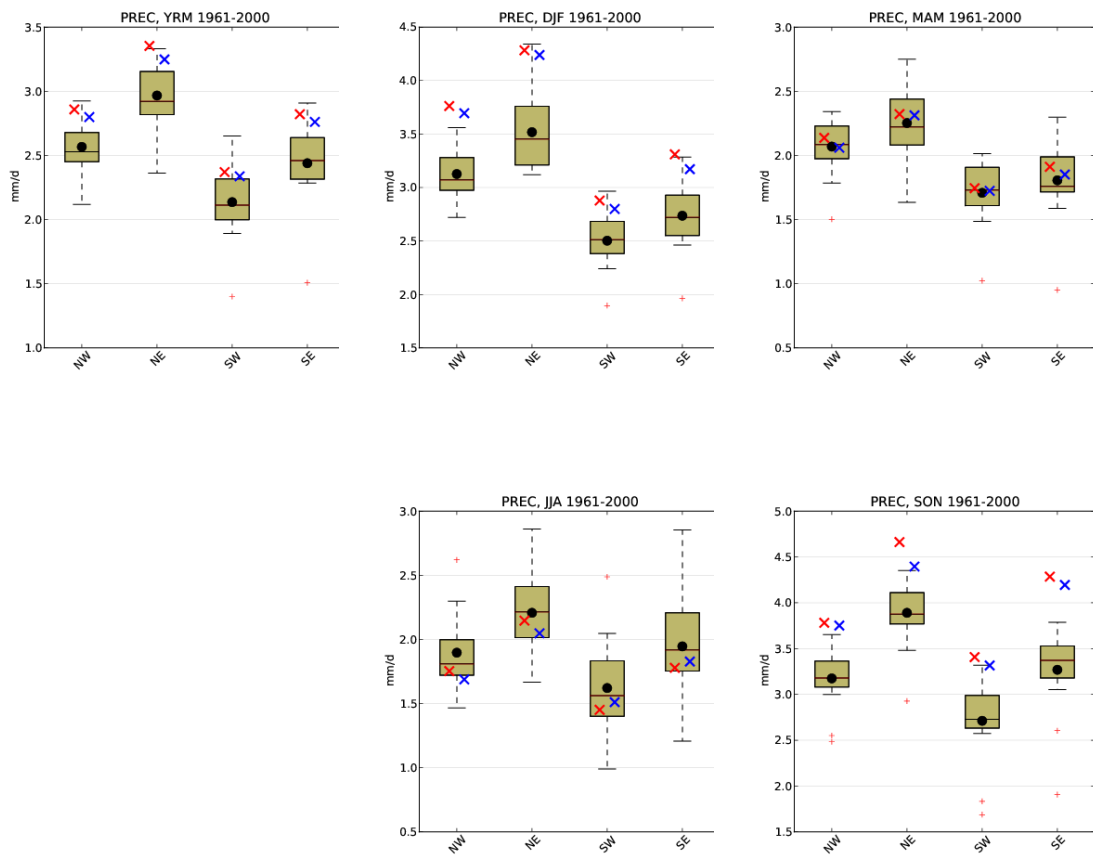


Figure 17: Similar as Fig. 15, for precipitation [mm/d].

On the coupling of the oceanic North Sea model HAMSOM with the regional atmospheric model REMO

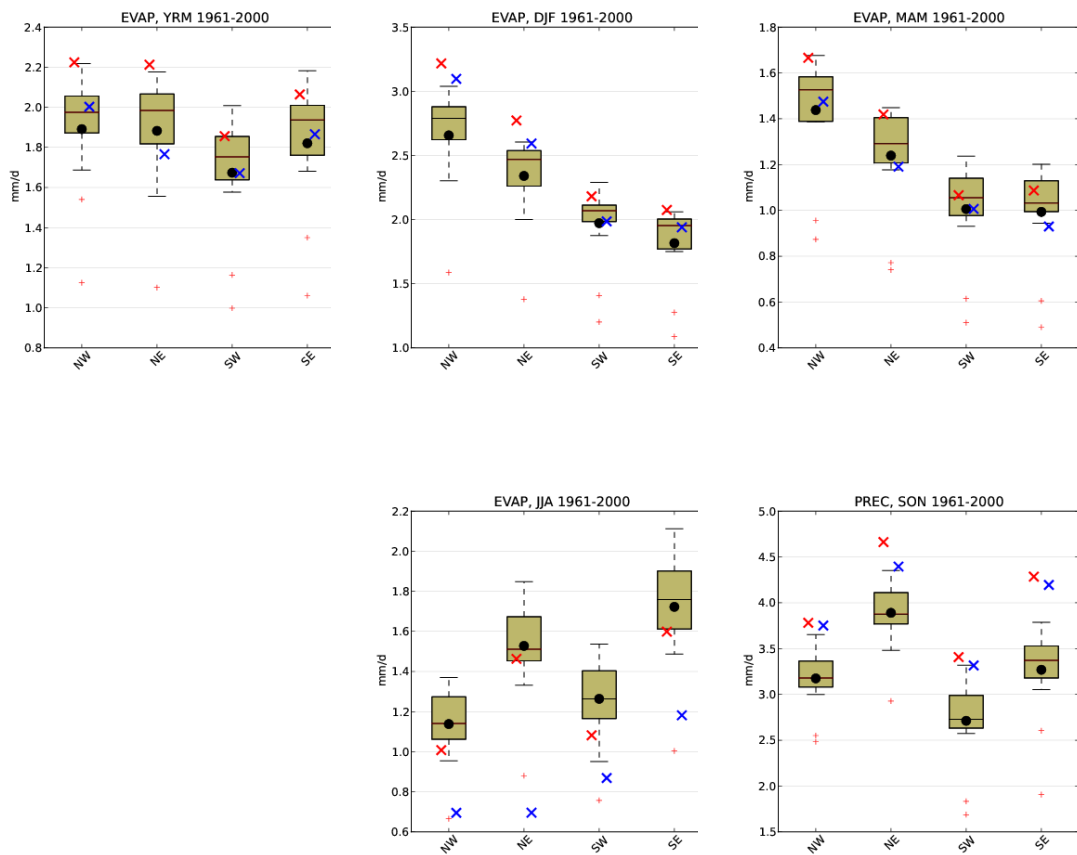


Figure 18: Similar as Fig. 15, for evaporation [mm/d].

On the coupling
of the oceanic
North Sea model
HAMSOM with
the regional
atmospheric
model REMO

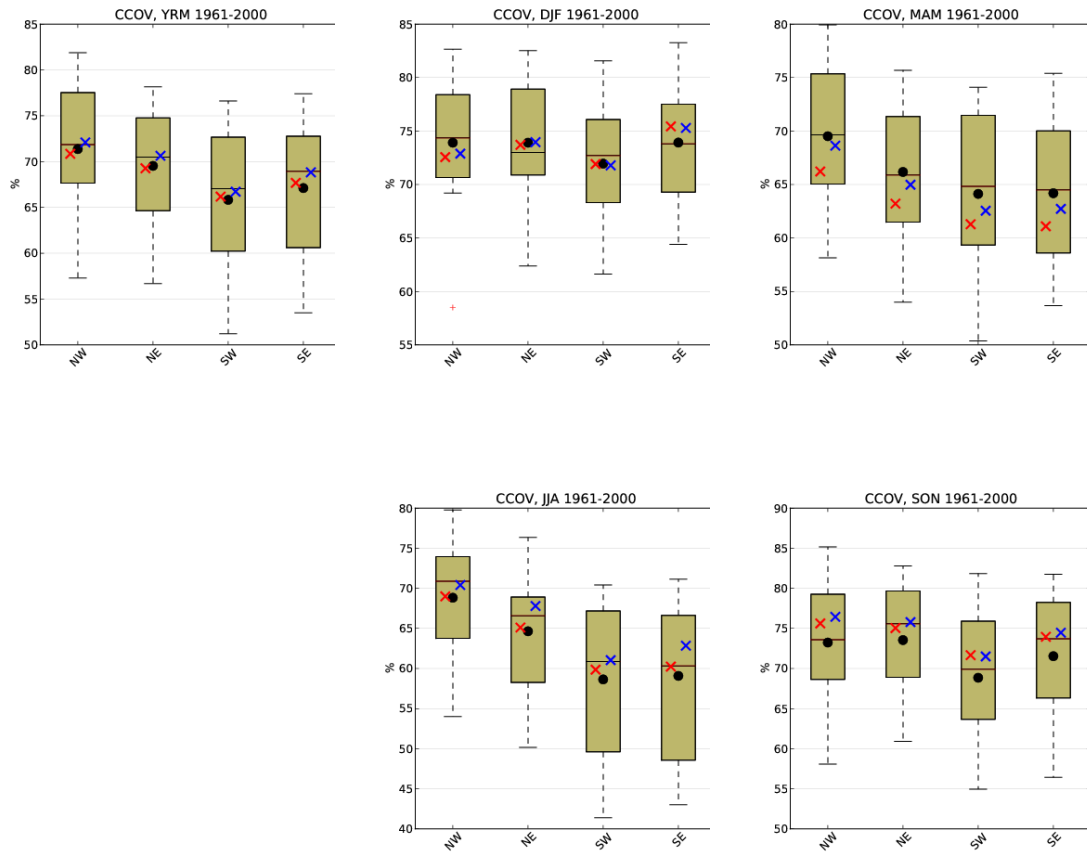


Figure 19: Similar as Fig. 15, for cloud cover [%].

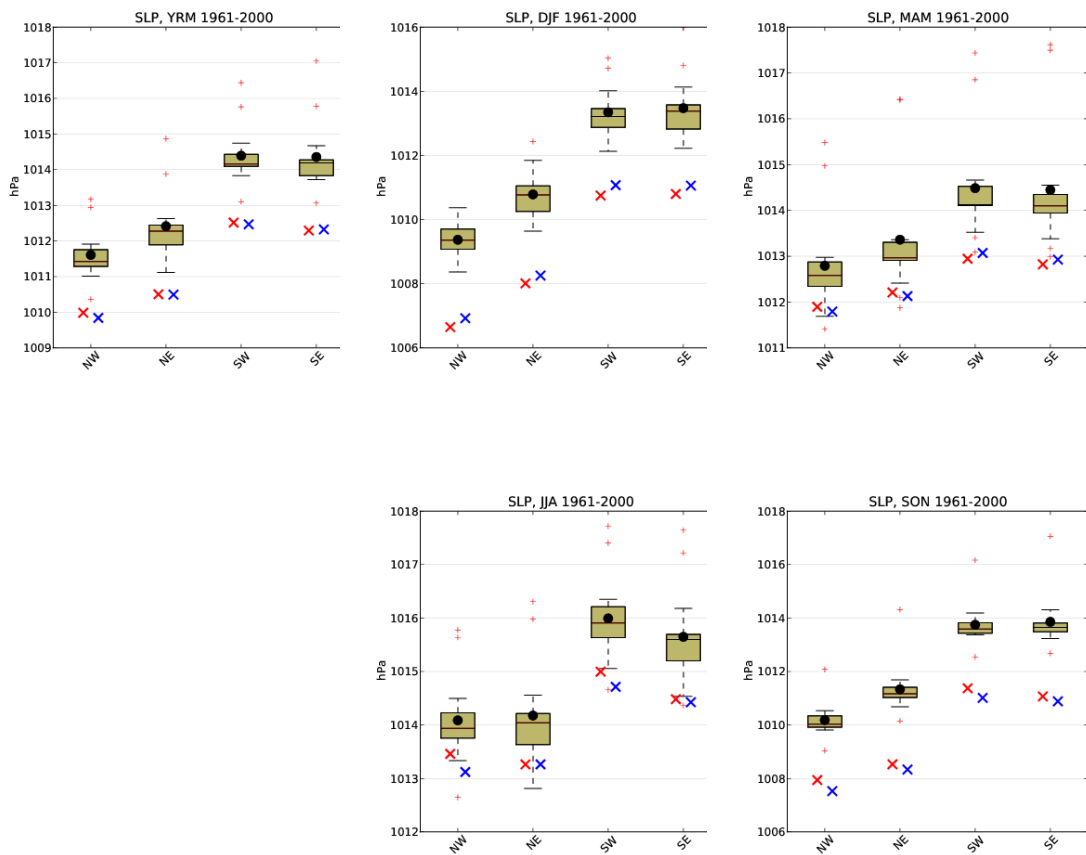


Figure 20: Similar as Fig. 15, for mean sea level pressure [hPa].

On the coupling of the oceanic North Sea model HAMSOM with the regional atmospheric model REMO

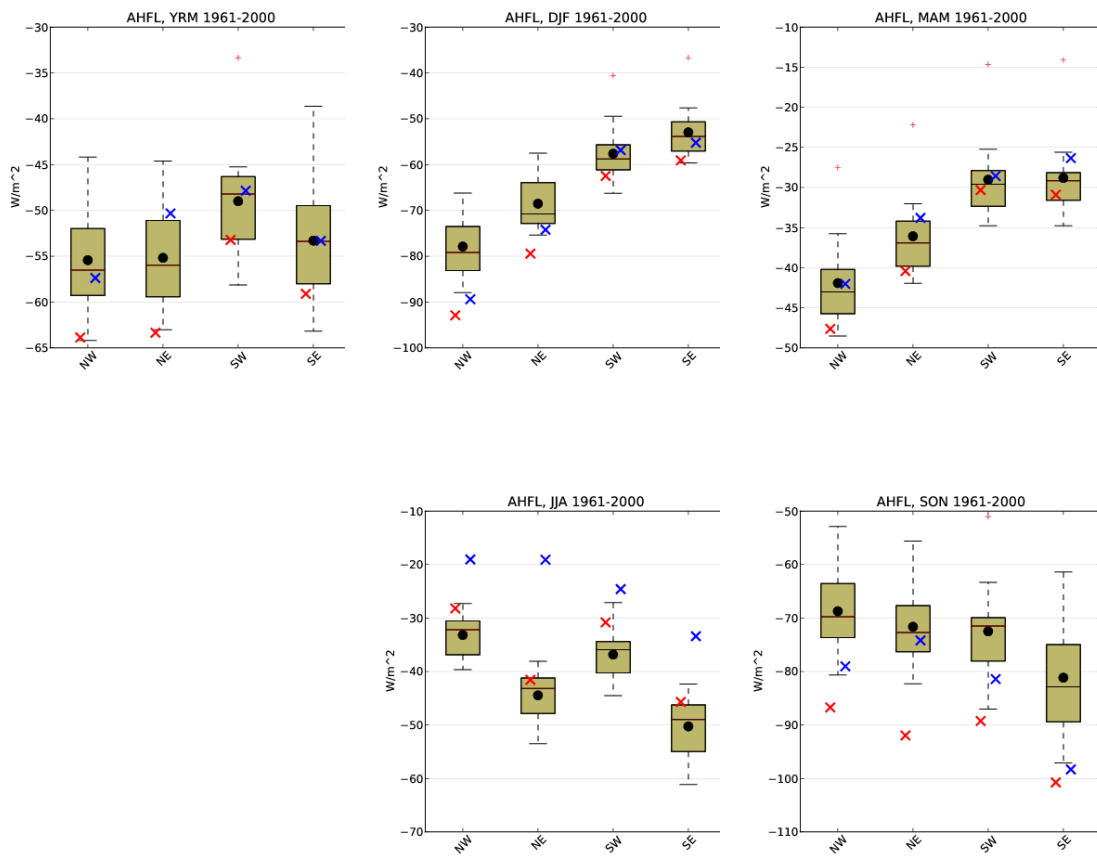


Figure 21: Similar as Fig. 15, for latent heat flux [W/m^2].

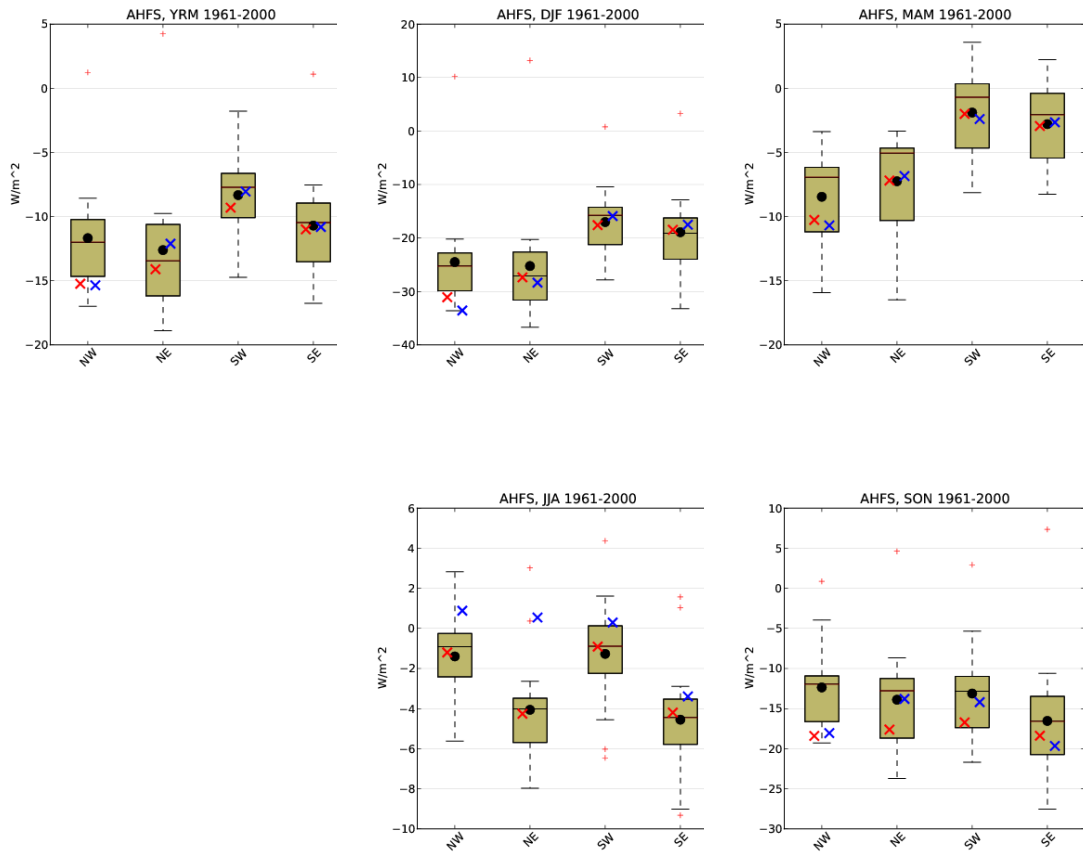


Figure 22: Similar as Fig. 15, for sensible heat flux [W/m^2].

On the coupling of the oceanic North Sea model HAMSOM with the regional atmospheric model REMO

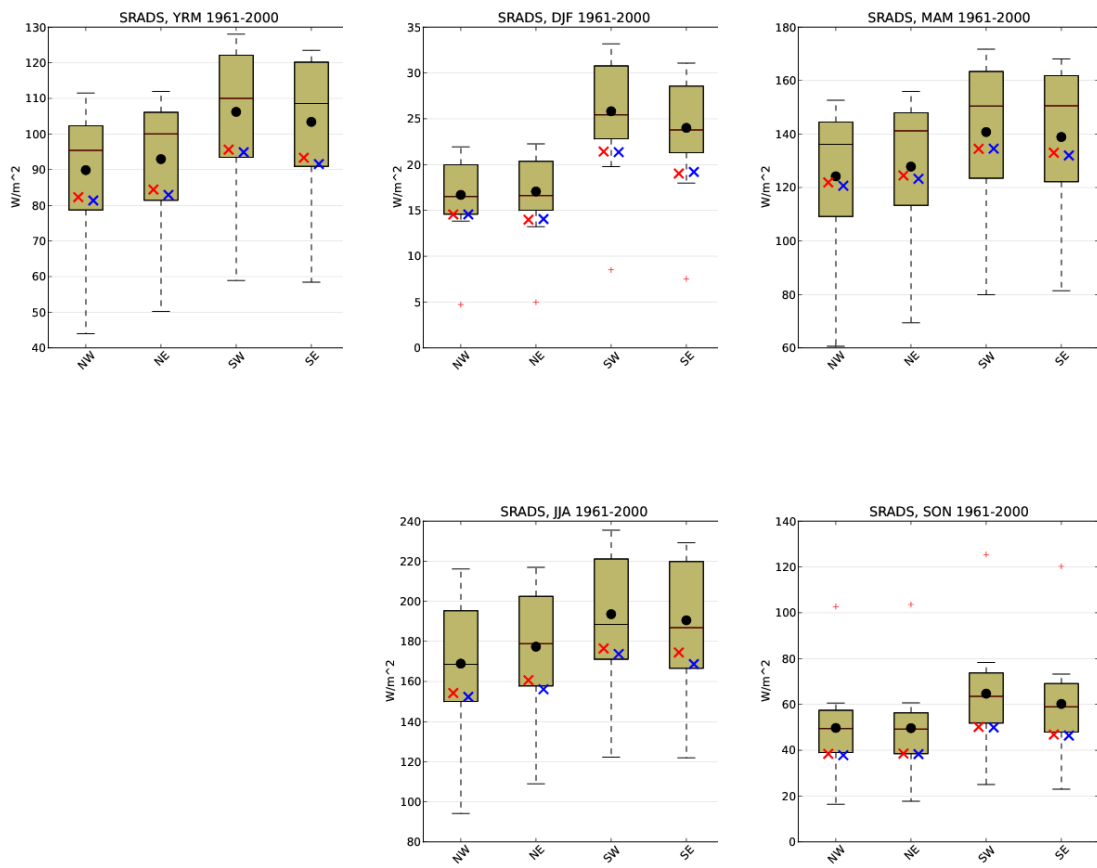


Figure 23: Similar as Fig. 15, for net surface solar radiation [W/m^2].

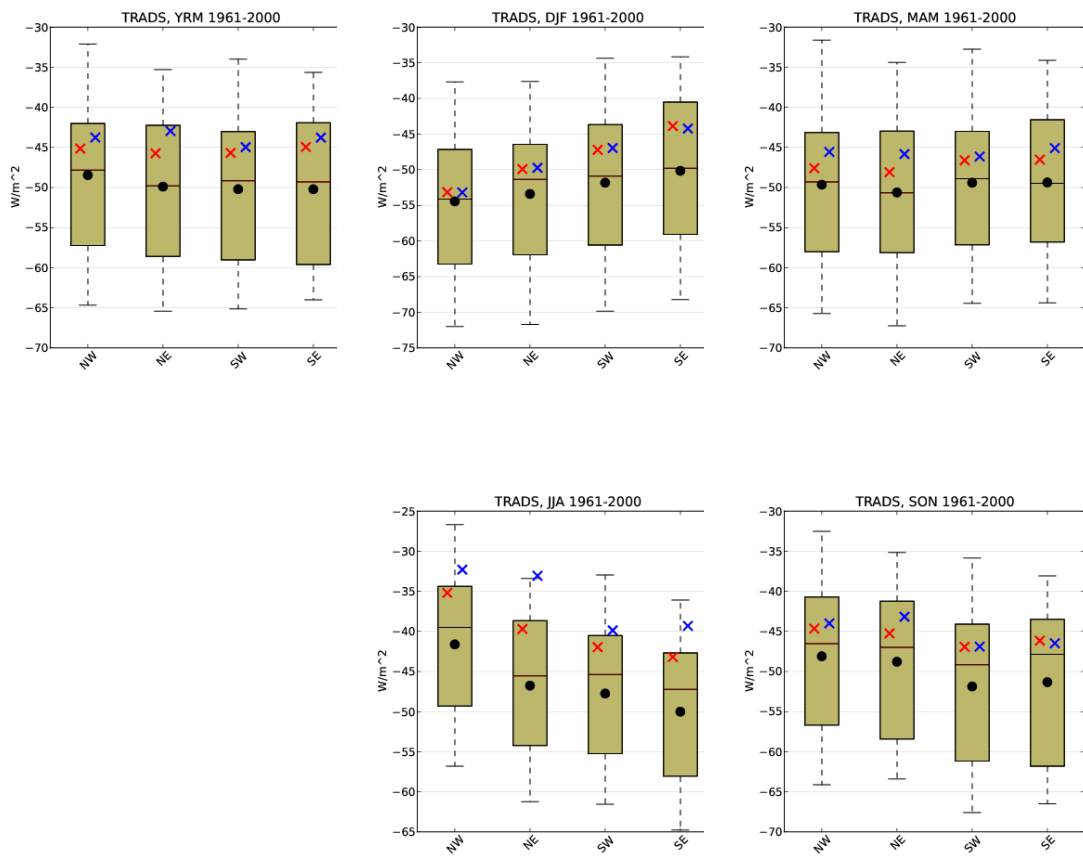


Figure 24: Similar as Fig. 15, for net surface thermal radiation [W/m^2].

6 Comparison of the coupled REMO/HAMSOM simulation with the other REMO simulations over the North Sea region

In Chapter 4 we gave a comparison of the uncoupled NCEP-driven REMO simulation CSC-022, the coupled NCEP-driven REMO/MPIOM simulation MPI-253, the coupled ECHAM5/MPIOM-driven REMO/MPIOM scenario simulation IfM-002 (only SST and cloud cover), and the uncoupled ERA40-driven REMO simulation CSC-300 with the reanalysis- and observational datasets. The coupled REMO/HAMSOM simulation IfM-201 and the uncoupled REMO simulation IfM-123 have not been included in the evaluation in Chapter 4. The reason is, that the effect of the REMO/HAMSOM coupling is locally constrained on the North Sea. Therefore, the differences between the forcing simulation MPI-253 and IfM-201 are better to compare in the North Sea region, while these differences would be hardly visible on the full-domain plots shown there. Similarly, the uncoupled simulation IfM-123 is forced by the ocean output of MPI-253, such that these two simulations should show the same climate, and differences between them can be attributed to model internal variability alone (see e.g. Laprise et al. 2012). Therefore simulation IfM-123 can serve as a reference to estimate the ratio between the signal of the REMO/HAMSOM coupling and mere random variability. In fact, we will see that the difference between IfM-123 and MPI-253 are smaller than between IfM-201 and MPI-253, even if locally constrained to the North-Sea region.

In this Chapter, the differences between the simulations IfM-201 and IfM-123 to the simulation which provides their forcing, MPI-253, are discussed. As already mentioned in Chapter 2, the simulations IfM-201 and IfM-123 are only available for the period 1987-1999, which was chosen because the SST cold bias of MPI-253 in the North Sea is relatively small in this period. Therefore, the comparison is shown for this period only. Since the differences are localized to the North Sea and its vicinity, the here presented horizontal plots show cuts for the North Sea region. No clear signal is seen for precipitation, cloud cover, and surface solar radiation. Although these quantities show some internal variability, the local effect of the coupling over the North Sea can not be distinguished from this variability. A possible reason is that these variables are related to cloud processes in the higher troposphere with no direct vicinity to the SST such that the effects are spread over a larger area and thus cannot be directly detected. Model output of sea level pressure and 2m dew point temperature is missing for IfM-201 and could therefore not be evaluated. The results show, that the effect of the REMO/HAMSOM coupling mainly affects the regions near to the coastlines of the North Sea, and the western edge of the Baltic Sea.

In the following a list of all variables is given for which a local effect of the coupling of the local ocean is seen:

- **Sea surface temperature** (Fig. 25): Since the SST is directly calculated by HAMSOM, it is not surprising that significant differences between the coupled REMO/HAMSOM simulation IfM-201 and the driving simulation MPI-253 are seen. In autumn and winter, HAMSOM simulates lower SST, especially near the coast lines. In contrast, in summer the simulated SST is higher close to the southern coast line. A dipole-like structure on the North, with higher SST north of 60°N and lower south of this line, is probably caused by an interpolation of the ocean forcing in HAMSOM (T. Pohlmann, personal communication). Note that the SST of IfM-123 is identical to MPI-253, therefore it is not shown. IfM and BSH have done a more detailed analysis of the HAMSOM simulations.
- **2m temperature** (Fig. 26): The difference in surface near temperature between IfM-201 and MPI-253 closely follows the SST difference and leads to a cooling in winter, spring, and autumn especially near the coastal regions, and to a locally constrained warming at the German bight in summer up to 2 °C. The general cooling also extends to the surrounding land areas and is larger than the difference between IfM-123 and MPI-253.
- **Evaporation** (Fig. 27): The different SST leads to differences in evaporation between IfM-201 and MPI-253 which clearly exceed the differences between IfM-123 and MPI-253 expected from natural variability. It induces a decrease in autumn and winter, and an increase in summer near the southern coast, which also extend to the land areas.
- **Latent heat flux** (Fig. 28): The surface latent heat flux is a quantity, which is closely related to the evaporation. Therefore, the difference between IfM-201 and MPI-253 in both quantities look very similar quantitatively and in magnitude, but with opposite sign.
- **Sensible heat flux** (Fig. 29): The difference between IfM-201 and MPI-253 in the sensible heat flux is similar in sign as the latent heat flux, with an increase in autumn and winter, and a decrease in summer. The differences are largest close to the coastlines. However, the magnitude of the differences in sensible heat flux is smaller than for the latent heat flux.
- **Surface thermal radiation** (Fig. 30): In contrast to the net surface solar radiation, the coupling with HAMSOM shows an effect on the thermal radiation, which is larger than the difference of MPI-253 to the reference simulation IfM-201. Near the southern coast lines, IfM-201 has less thermal radiation (i.e. positive differences) than MPI-253 in winter, while it has more (negative differences) in summer.

On the coupling of the oceanic North Sea model HAMSOM with the regional atmospheric model REMO

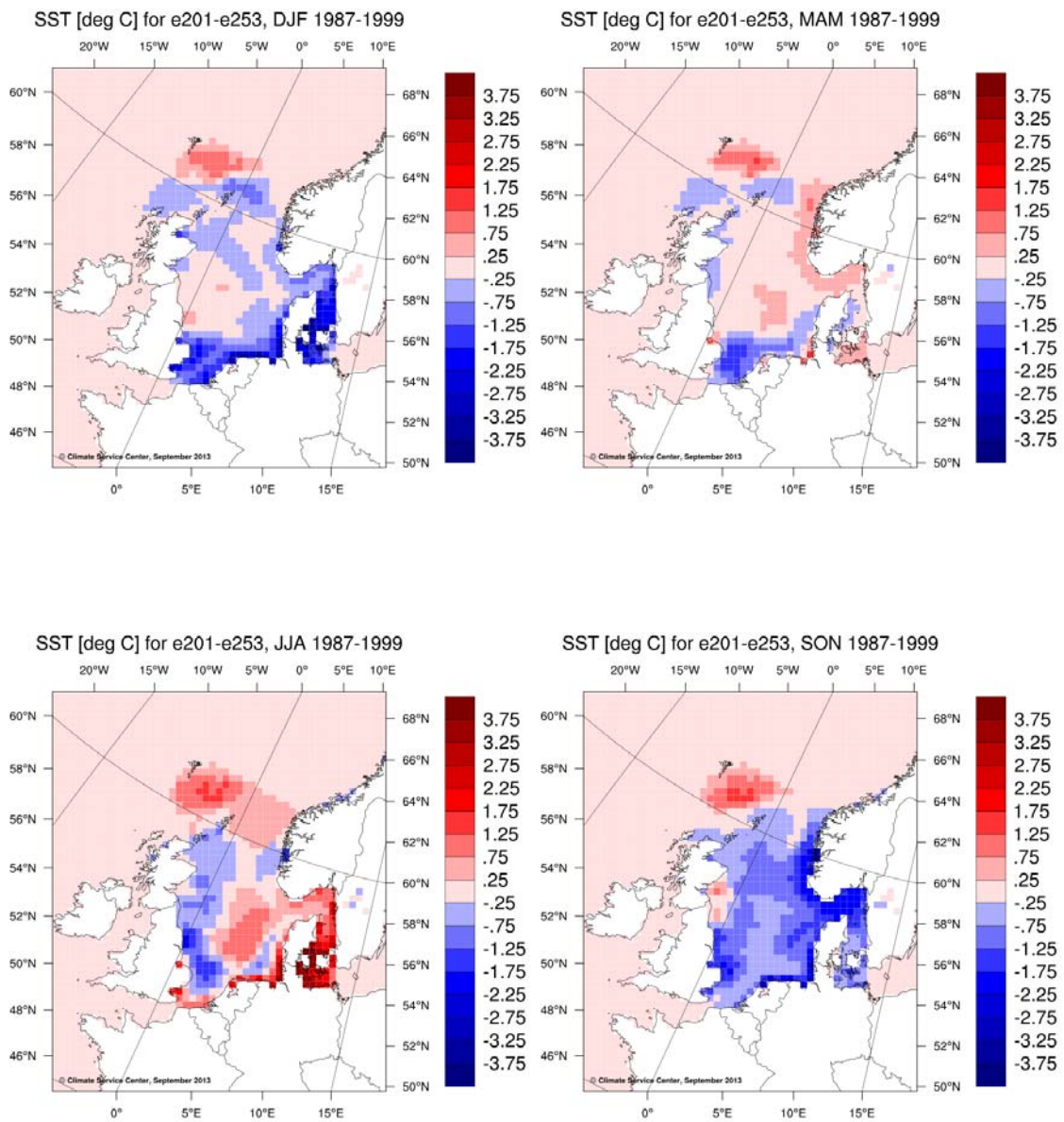


Figure 25: Sea surface temperature difference between IfM-201 and MPI-253 [°C]. Top left to bottom right: Seasons DJF, MAM, JJA, SON.

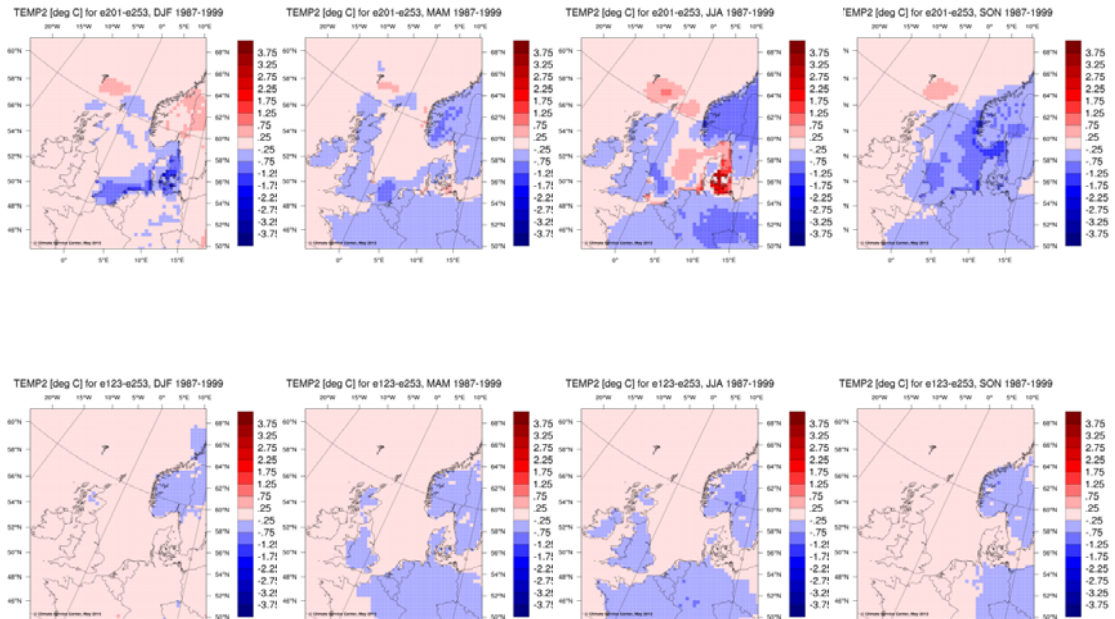


Figure 26: 2m air temperature difference between IfM-201 and MPI-253 (top) and IfM-123 and MPI-253 (bottom) [°C]. Left to right: Seasons DJF, MAM, JJA, SON.

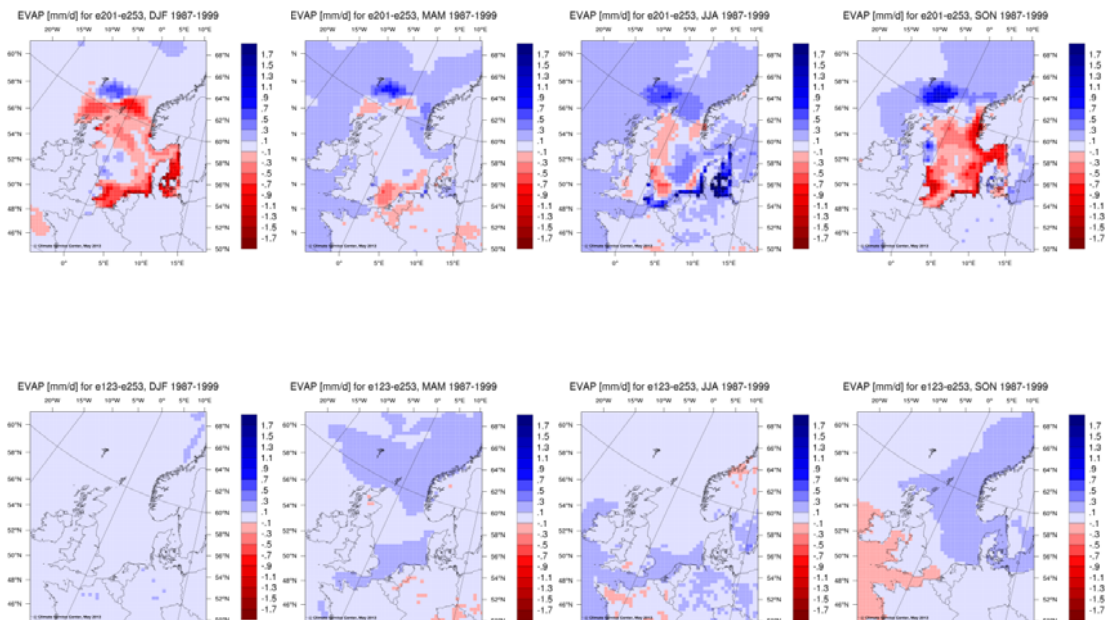


Figure 27: Evaporation difference between IfM-201 and MPI-253 (top) and IfM-123 and MPI-253 (bottom) [mm/d]. Left to right: Seasons DJF, MAM, JJA, SON.

On the coupling of the oceanic North Sea model HAMSOM with the regional atmospheric model REMO

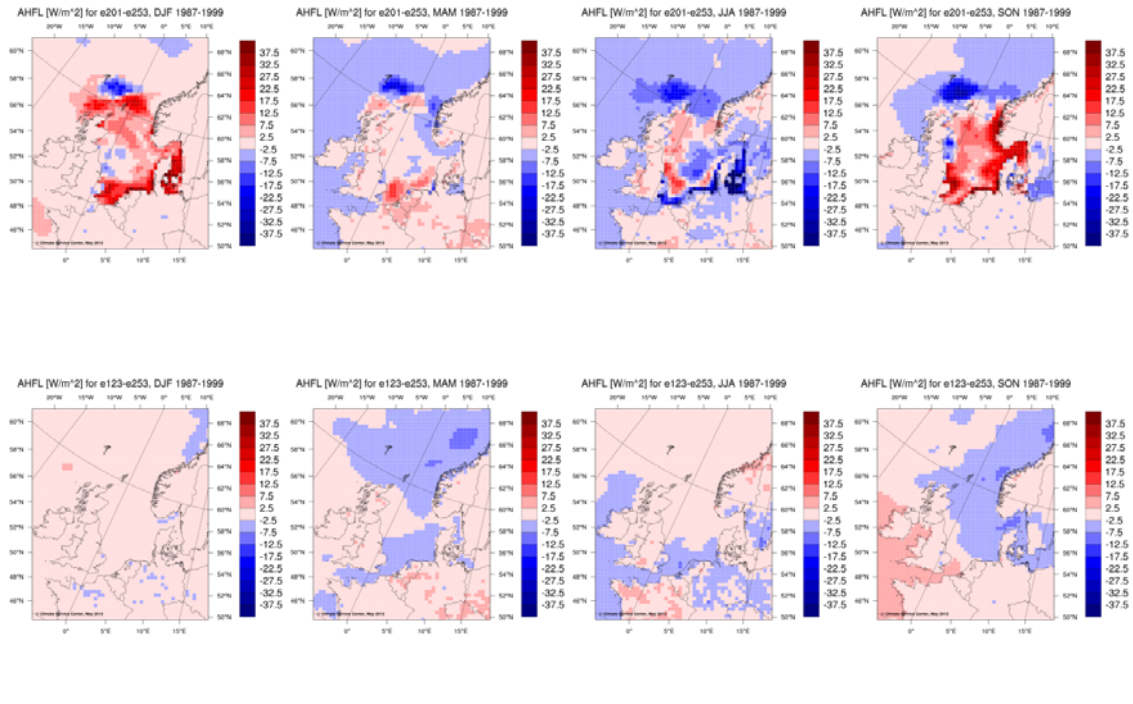


Figure 28: Latent heat flux difference between IfM-201 and MPI-253 (top) and IfM-123 and MPI-253 (bottom) [W/m^2]. Left to right: Seasons DJF, MAM, JJA, SON.

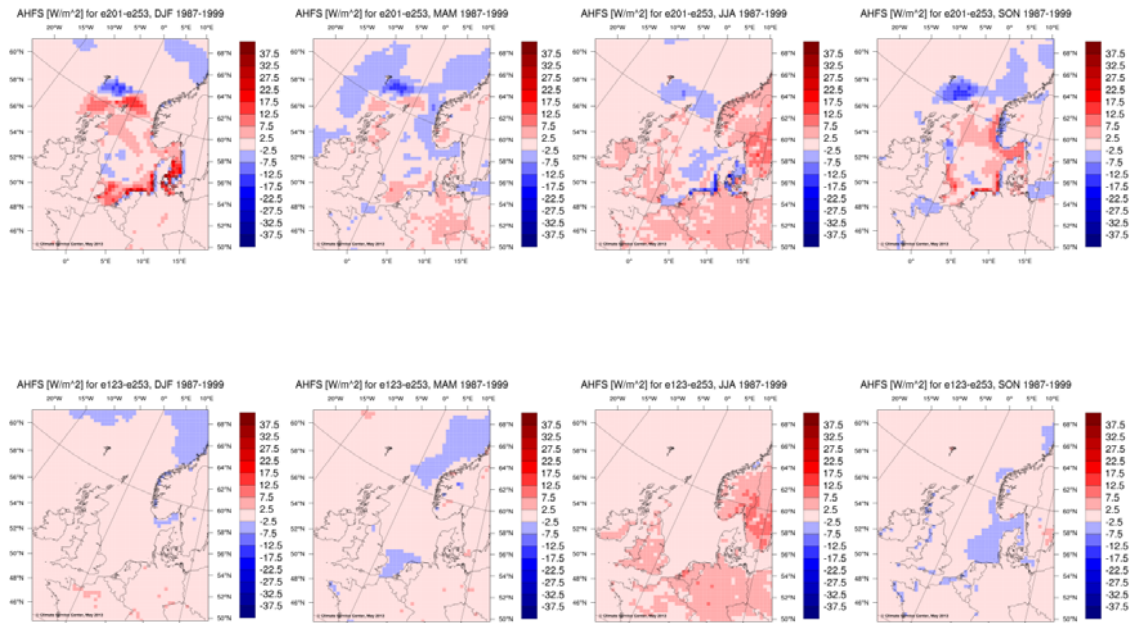


Figure 29: Sensible heat flux difference between IfM-201 and MPI-253 (top) and IfM-123 and MPI-253 (bottom) [W/m^2]. Left to right: Seasons DJF, MAM, JJA, SON.

On the coupling of the oceanic North Sea model HAMSOM with the regional atmospheric model REMO

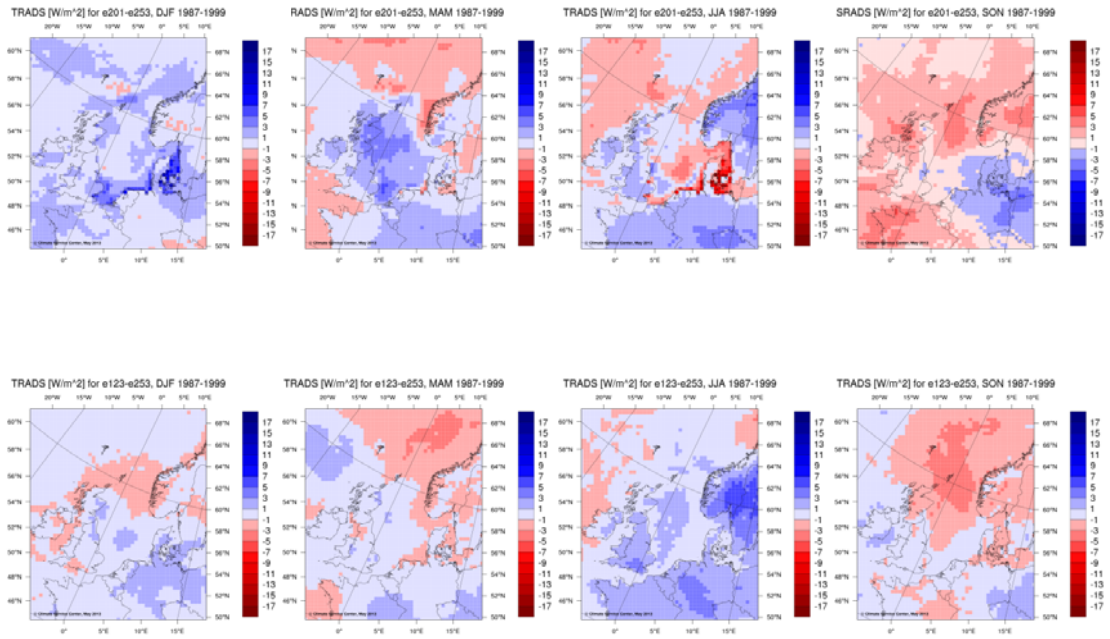


Figure 30: Surface thermal radiation difference between IfM-201 and MPI-253 (top) and IfM-123 and MPI-253 (bottom) [W/m^2]. Left to right: Seasons DJF, MAM, JJA, SON.

7 Conclusion

In this report, a validation and discussion of the coupled and uncoupled simulations described in Chapter 2, has been discussed. Three different models have performed them: The uncoupled REMO (CSC-022, CSC-300, IfM-123, all with different model versions), a coupled REMO/MPIOM system (MPI-253), and coupled REMO/HAMSOM system (IfM-201, IfM-002). The differences among the model simulations can be attributed to the different atmospheric and oceanic forcing fields (NCEP, ERA40, ECHAM5/MPIOM), and the different models and model versions. In general, it can be stated that the biases of most of the studied atmospheric climate variables are similar for all simulations, and can therefore be explained by typical biases of the REMO model which are present in all coupled and uncoupled model versions. However, some quantities show some sensitivity to the differences in simulated SST of the coupled model versions, to the prescribed SSTs from the reanalysis data, especially over the ocean. However, there are also considerable differences between the observational datasets which are partly in the same order of magnitude as the differences between the simulations and the observations, making clear statements about the model bias difficult.

The most obvious feature of the analyzed simulation ensemble is the SST cold bias of the coupled REMO/MPIOM simulation MPI-253 in the GIN seas, leading to an increased sea ice cover in the Arctic, and leads to a too low SST into the North Sea. The ECHAM5/MIPOM forced C20-simulation IfM-002 shows a very similar SST bias, leading to similar consequences on the atmospheric variables, and is therefore not shown everywhere. This emphasizes the speculation that this bias is mainly caused by flaws in the REMO/MPIOM coupling system rather than a problem with the forcing fields.

A comparison of MPI-253 with the uncoupled NCEP-SST forced simulation CSC-022 shows, that the SST bias affects the 2m air temperature over the ocean, leading to clearly lower temperatures over the North Sea in comparison with the ENSMBLES simulations. Over the land areas, mainly Scandinavia is affected, while 2m temperature biases are similar in the rest of Europe. Another affected quantity is the evaporation: While the uncoupled reference simulation rather tends to have more evaporation over the North Sea in the yearly mean than the observational datasets and the ENSMBLES simulations, there is a clear low-evaporation bias of the REMO/MPIOM simulations in the region in summer. The SST cold bias further leads to reduced heat fluxes, especially in summer. In the other seasons, this effect partly compensates a too high latent heat flux of the uncoupled simulation in the North Sea region.

The so far mentioned surface-near climate variables are closely affected by the SST, while precipitation, cloud cover, solar radiation, and sea level pressure are less sensitive to changes in the SST. Regarding precipitation, REMO has a general wet bias, both over ocean and over land, which is also seen within the intercomparison with the ENSMBELS simulations over the North Sea. It is strongest in winter and weaker in summer. However, this bias is hardly affected by the SST cold bias, and can thus be attributed mainly to the atmospheric parameterizations rather than the coupling. REMO simulated cloud cover is larger compared to ERA40 over ocean, but smaller over Europe, but differences among the REMO simulations are small, while on the other hand the ENSEMBLES ensemble shows a large band width of cloud cover over the North Sea. A quantity, which is closely related to the cloud cover, is the net surface solar radiation, which is systematically too low in REMO. It is compensated by a too low thermal radiation. This bias is much larger than the differences between the coupled and uncoupled simulations. However, there is also a large spread in radiation of the ENSEMBLES simulations, showing that REMO is not the only RCM with a problem in radiation. Further, REMO shows a low pressure bias in mean sea level pressure, relative to the observations as well as the ENSEMBLES ensemble, which is consistent for all REMO simulations and depends on the forcing dataset and domain size rather than differences in SST.

The coupled REMO/HAMSOM simulation IfM-201 is forced by the SST and sea ice output of MPI-253, such that a comparison of these two simulations can give insight to the impact of the coupling of REMO and HAMSOM. A third uncoupled REMO simulation IfM-123, was included to the evaluation in order to distinguish between the signal of the coupling and mere random internal model variability. The effect of the coupling on the atmospheric variables turns out to be locally constrained to the North Sea, the western part of the Baltic Sea, and the surrounding land areas. It is mainly driven by the SST differences between IfM-201 and MPI-253, which are largest in the coast-near areas of the North Sea. It leads to a general cooling in 2m temperature with a slight warming in summer, a decrease in evaporation and latent heat flux in winter and increase in summer, and less net thermal radiation in winter and more in summer. No clear signal is seen for the quantities which are mainly caused by processes in the higher troposphere like precipitation, cloud cover, and net surface solar radiation.

For further studies, it can be recommended to force the coupled REMO/HAMSOM model with an improved REMO/MPIOM modeling system which is currently under development (Sein et al. 2013), to answer the question if the effects of the REMO/HAMSOM coupling at the coast-near regions are robust in magnitude to improved SST values. Since these effects are very local, it might be necessary to use very high resolved observational datasets in the region to analyze the improvements of the description of the atmosphere coming from the regional coupled model.

References

- Bülow, K., A. Ganske, H. Heinrich, S. Hüttl-Kabus, B. Klein, H. Klein, J. Möller, G. Rosenhagen, N. Schade and B. Tinz (2013) Comparing meteorological fields of the ENSEMBLES regional climate models with ERA-40-data over the North Sea. KLIWAS Schriftenreihe 21-2013, DOI: 10.5675/Kliwas_21.2013_ERA40data.
- Jacob D., K. Bülow, L. Kotova, C. Moseley, J. Petersen and D. Rechid (2012) Regionale Klimaprojektionen für Europa und Deutschland: Ensemble-Simulationen für die Klimafolgenforschung. CSC Report 6, Climate Service Center, Hamburg. (http://www.climate-service-center.de/imperia/md/content/csc/csc_report6.pdf)
- Jungclaus J.H. *et al.* (2006) Ocean Circulation and Tropical Variability in the Coupled Model ECHAM5/MPI-OM. *J. Climate*, 19, 3952–3972.
- Laprise, R. *et al.* (2012): Considerations of Domain Size and Large-Scale Driving for Nested Regional Climate Models: Impact on Internal Variability and Ability at Developing Small-Scale Details. *Climate Change*, DOI 10.1007/978-3-7091-0973-1_14
- Pohlmann, T., (2006) A meso-scale model of the central and southern North Sea: consequences of an improved resolution. *Continental Shelf Research* 26, 2367 – 2385
- Schrum, C., U. Hübner, D. Jacob, R. Podzun (2003) A coupled atmosphere/ice/ocean model for the North Sea and the Baltic Sea. *Climate Dynamics* 21: 131-151
- Sein, D. V., Mikolajewicz U., Gröger M., Maier-Reimer E., Fast I., Hagemann S. (2013) Regionally coupled atmosphere-ocean-sea ice-marine biogeochemistry model REMO/MPIOM/HAMOCC. Downscaling of future climate change A1B scenario for the North Atlantic and North European shelves. *In preparation*
- Su J., Yang H., Moseley C., Elizalde A., Sein D., Pohlmann T. (2013) Ocean feedback mechanism in a coupled atmosphere-ocean model system for the North Sea. In prep to submit to *Tellus A*.
- Tomassini, L., and Elizalde, A. (2012) Does the Mediterranean Sea influence the European summer climate? The anomalous summer 2003 as a testbed. *J. Climate* 25, 7028-7045
- van der Linden, P., Mitchell J.F.B. (eds.) (2009) ENSEMBLES: Climate Change and its Impacts: Summary of research and results from the ENSEMBLES project. Met Office Hadley Centre, FitzRoy Road, Exeter EX1 3PB, UK, 160.



Bundesanstalt für Wasserbau
Kompetenz für die Wasserstraßen

Bundesanstalt für Wasserbau (BAW)

Kußmaulstraße 17
76187 Karlsruhe

www.baw.de
info@baw.de

Bundesamt für Seeschifffahrt und Hydrographie (BSH)

Bernhard-Nocht-Straße 78
20359 Hamburg

www.bsh.de
posteingang@bsh.de



**BUNDESAMT FÜR
SEESCHIFFFAHRT
UND
HYDROGRAPHIE**



Deutscher Wetterdienst (DWD)

Frankfurter Straße 135
63067 Offenbach/Main

www.dwd.de
info@dwd.de

**Bundesanstalt für
Gewässerkunde (BfG)**

Am Mainzer Tor 1
56068 Koblenz

www.bafg.de
posteingang@bafg.de



IMPRESSUM

Herausgeber:

Bundesanstalt für Gewässerkunde
KLIWAS Koordination
Am Mainzer Tor 1
Postfach 20 02 53
56002 Koblenz
Tel.: 0261 / 1306-0
Fax: 0261 / 1306-5302
E-Mail: kliwas@bafg.de
Internet: <http://www.kliwas.de>

Redaktion: KLIWAS-Koordination,
Bundesanstalt für Gewässerkunde

Autoren: Christopher Moseley, Daniela Jacob,
BSH and CSC

Layout: Christin Hantsche und Tobias Knapp,
Bundesamt für Seeschifffahrt
und Hydrographie - Rostock

Druck: Bundesanstalt für Gewässerkunde

DOI: 10.5675/Kliwas_63/2014_REMO_HAMSOM_2